ARTICLE TEMPLATE

A climate-based metapopulation malaria model with human travel and treatment

Baaba A. Danquah[a] , Faraimunashe Chirove[b] and Jacek Banasiak[c,d]

[a]Department of Mathematics and Statistics, University of Energy and Natural Resources, P. O. Box 214, Sunyani, Ghana; [b]Department of Mathematics, University of Johannesburg, Johannesburg, South Africa; [c]Department of Mathematics and Applied Mathematics, University of Pretoria, Pretoria, South Africa;[d]Institute of Mathematics, Łódź University of Technology, Łódź, Poland

ARTICLE HISTORY
Compiled December 9, 2024

ABSTRACT
A climate-based metapopulation malaria model is formulated by incorporating human travel between zones with varying climatic factors, effective and counterfeit drug treatments, and time-periodic parameters for the mosquito population to understand the effect of human travel on malaria transmission. We study the existence, uniqueness, and stability of positive periodic solutions in the model and carry out numerical simulations for three climatic zones of Ghana. The study shows that the climate effects introduce fluctuations in the solutions, while human travel between zones affects the disease prevalence in each zone and the local transmission dynamics of malaria. We observed different outcomes depending on various restrictions imposed on human travels. The study also suggests that it is essential to ban the sale, importation or manufacture of counterfeit drugs and punish the offenders to ensure the effective use of high-quality drugs in the population.

KEYWORDS
Malaria transmission; metapopulation; non-autonomous model; reproduction ratio; uniform persistence

1. Introduction

Malaria is a vector-borne disease caused by five species of the parasite of the genus *Plasmodium*, transmitted through infected female *Anopheles* mosquitoes, the deadliest of the species being *Plasmodium falciparum* [3]. Despite the decline in *P. falciparum* malaria infections due to the massive deployment of control tools since the year 2000, the disease continues to burden the public health and the economies of the endemic countries in Africa [1]. The World Health Organization (WHO) reports that of the 627,000 malaria deaths worldwide in 2020, almost 96% were in Africa [1]. Some of these deaths have been a result of the use of counterfeit drugs by a significant proportion of infected humans, including children under five years [4, 5, 7, 8].

The malaria transmission intensity and incidence in sub-Saharan Africa have been linked to the climate conditions such as rainfall, temperature and humidity that increase the mosquito densities, distribution and the transmission capacity [9–13].

CONTACT B. A. Danquah. Email: babghans@gmail.com

Malaria transmission was also found to vary due to the spatio-temporal heterogeneity of the environment [4, 11, 14–21], the type of parasites and vectors, including the chemoresistant ones [22], the socio-economic conditions [19, 20, 23, 24], and movement of humans [25], just to mention a few. For instance, different ecological zones of Ghana, a malaria-endemic country in West Africa, experience varying mosquito densities and distribution as well as malaria morbidity patterns [15, 18, 20, 21, 26, 27]. Additionally, malaria transmission in urban areas is usually lower than in rural, peri-urban areas due to the availability of control interventions [11, 18, 20].

A strong association has been found between malaria infections and a recent trip to rural areas by urban dwellers [23, 28]. Since the mosquito flight studies, [29, 30], indicate that most female mosquitoes travel only a few kilometres during their lives and thus may spend their lifetime in or around the houses where they emerge as adults, it is more likely that humans, rather than mosquitoes, usually carry the malaria parasites over long distances and thus are responsible for the correlations between the above mentioned trips and infections. In other words, human movement between spatially heterogeneous environments with malaria prevalence not only impacts the translocation of infections but also affect the local disease transmission dynamics and control efforts as well.

To study the spread and control of infectious diseases across spatially heterogeneous environments caused by human migrations has been carried out using metapopulation models [31–36]. Such models are well suited to study the role played by human and vector mobility between regions with different environments or socioeconomic conditions in the persistence, spread and sometimes reintroduction of diseases [36]. In [37], the authors studied the effect of human movement, especially of asymptotic carriers, on the spread of malaria and the impact of spatial heterogeneities on the control strategies. In [32, 33] the authors used metapopulation setting to describe how the movement of both hosts and vectors can be modelled, to understand the effect of host movements on the persistence of malaria in low transmission regions, and also to explore control strategies in a heterogeneous environment. The impact of different malaria patterns in the areas of heterogeneous transmission characteristics on determining effective targeted intervention strategies is addressed in [38]. A study investigating transmission dynamics in a patchy environment was also conducted in [34].

Recent evidence has shown that high malaria transmission is observed at the beginning of heavy rains due to the high impact of the rainfall and high temperature on the mosquito density and sporozoite rates [14, 15]. On the other hand, excessive rainfalls flush out mosquito breeding sites, leading to the transmission reduction [12] in sub-Saharan Africa, showing strong dependence of malaria transmission on climatic factors. This dependence in a single homogeneous environment has been explored in [12, 13, 39–43]. In particular, [12, 13] studied the effect of rainfall and temperature on mosquito population dynamics, malaria invasion, persistence and local seasonal extinction, and the impact of seasonality on malaria transmission has been investigated in, while [39] and [40–42] used climate-based models that incorporated the juvenile stage of the mosquitoes to investigate, respectively, the effect of periodic biting rate and the impact of climatic factors like the rainfall and the temperature on the dynamics of malaria transmission; the effect of global climate change on it was modelled in [43]. Further, a periodic Ross-Macdonald malaria model that considers the effect of temporal and spatial heterogeneity on disease transmission was proposed in [45] to explore the effect of travel control on disease prevalence.

This paper proposes a metapopulation model incorporating climatic factors such as rainfall and temperature and ineffective/counterfeit and effective treatments to study

how human migrations across heterogeneous environments impact malaria transmission and control. We extend the homogeneous malaria models developed in [72, 73] (which notably feature asymptomatic carriers of infection) by considering counterfeit drug users [46], human travel from one region to another and the temperature and rainfall dependent parameters in the mosquito populations. The paper is organized as follows. Section 2 describes the model with the temperature- and rainfall-dependent parameters. A mathematical analysis of the non-autonomous system is presented in Section 3. In Section 4, we establish the threshold dynamics of the model in terms of the reproduction ratio R_0 by using the next generation operator method [48]. The infected classes are shown to be uniformly persistent in Section 5. In Section 6, we consider a special case of the three ecological zones of Ghana and explore how human travel between these heterogeneous environments affects the disease dynamics. The discussion of the results is done in Section 7.

2. Model Formulation

We consider the spatial spread of malaria in n ecological zones, which have varying temperature and rainfall patterns, access to counterfeit drugs, and are connected by human movement. The total human and female anopheles mosquito population sizes in each region $i = 1, ..., n$, are denoted by $N_{h,i}(t)$ and $N_{m,i}(t)$, respectively. For each region i at time t, the total human population is divided into four epidemiological classes, susceptibles, infectious, users of counterfeit antimalarial drugs and users of effective antimalarial drugs denoted by $S_{h,i}(t)$, $I_{h,i}(t)$, $U_{h,i}(t)$ and $T_{h,i}(t)$ respectively, so that, $N_{h,i}(t) = S_{h,i}(t) + I_{h,i}(t) + U_{h,i}(t) + T_{h,i}(t)$, while the mosquito population is divided into two classes, susceptibles $S_{m,i}(t)$ and infectious $I_{m,i}(t)$, so that, $N_{m,i}(t) = S_{m,i}(t) + I_{m,i}(t)$. The total human and mosquito populations $N_h(t)$ and $N_m(t)$ at a given time t are given by $N_h(t) = \sum_{i=1}^{n} N_{h,i}(t)$ and $N_m(t) = \sum_{i=1}^{n} N_{m,i}(t)$, respectively.

For each region $i = 1, ..., n$, the total birth rate of the human population is $\alpha_{h,i}$, and the natural per capita death rate is given by $\mu_{h,i}$. The susceptible humans have neither merozoites or gametocytes in their bodies nor immunity against malaria. They get exposed to malaria parasites at a force of infection of humans $\lambda_{h,i} = \frac{a_i \beta_{h,i} I_{m,i}}{N_{h,i}}$, where $\beta_{h,i}$ is the transmission probability from infectious mosquitoes to humans and a_i is the average number of bites per human in region i per unit time. The infectious humans survived the average latent duration $n_{h,i}$ with probability $p^{(h,i)} = e^{-\mu_{h,i} n_{h,i}}$ to show clinical symptoms of malaria and who can infect feeding mosquitoes. The infectious humans can be fully cured of malaria at the rate $\gamma_{h,i}$ due to the use of effective antimalarial drug(s) or become asymptomatic at the rate $\eta_{h,i}$ due to the use of counterfeit drug(s)(or naturally) or die at the disease induced death rate $\delta_{h,i}$. The users of counterfeit drugs are asymptomatic and can infect mosquitoes (at a lower rate compared to the infectious human), can recrudesce at rate $\xi_{h,i}$ into the infectious class or, in the case of adults, become susceptible at the rate $\theta_{h,i}$ due to the boosted immunity resulting from repeated exposures or semi-immunity [49, 72, 73]. The users of effective antimalarial drugs have been cured of malaria, have post-treatment prophylaxis and become susceptible at rate $\phi_{h,i}$ when this post-treatment prophylaxis wanes [49].

In the case of the mosquitoes, they are recruited at the per capita rate $\alpha_{m,i}(1 - \frac{N_{m,i}}{K_i})$, where $\alpha_{m,i}$ is the rate at which a larva becomes an adult, K_i is the larval carrying capacity, and $\mu_{m,i}$ represents the natural death rate of the mosquitoes [50]. The susceptible mosquitoes have no sporozoites in their body and are exposed to gametocytes

from infected humans at a force of infection of mosquitoes $\lambda_{m,i} = \frac{b_i \beta_{m,i}(I_{h,i}+\pi_i U_{h,i})}{N_{h,i}}$, where $\beta_{m,i}$ is the transmission probability from infected humans to mosquitoes, b_i is the mosquito biting rate in region i, and $0 < \pi_i < 1$ is the degree of infectiousness of the users of counterfeit drugs. The probability of the mosquito to survive the average latent duration $n_{m,i}$ to become infectious is given by $p^{(m,i)} = e^{-\mu_{m,i} n_{m,i}}$. It is assumed that the infective stage of the mosquitoes ends with their death due to their short life cycle.

Merozoites are the parasites released into the human bloodstream when a hepatic or erythrocytic schizont bursts and gametocytes are the sexual stages of malaria parasites that infect *Anopheline* mosquitoes when taken up during the blood meal [49]. Sporozoites are the motile malaria parasites that are infective to humans, inoculated by feeding female *Anopheline* mosquitoes, that invade the hepatocytes [49].

To account for migrations, we assume that only humans [32, 33, 37] can travel long distances between regions, so that, for each region $i = 1, ..., n$, $c^S_{i,j}$, $c^I_{i,j}$, $c^U_{i,j}$, $c^T_{i,j}$ are the travel rates from region j to region i of susceptibles, infectious, users of counterfeit antimalarial drugs and users of effective antimalarial drugs, respectively. We let $C^\Pi = [c^\Pi_{i,j}]$ with $\Pi = S, I, U, T$ be the travel rate matrices. As described in [34, 51], we assume that matrices $C^\Pi, \quad \Pi = S, U, T$, are irreducible and $c^\Pi_{ii} = 0$ for $\Pi = S, I, U, T$, and $i = 1, ..., n$.

The temperature (Γ) and rainfall (R) dependent parameters b_i, $\mu_{m,i}$ and $\alpha_{m,i}$ are discussed in [52] and [12], respectively, and expressed as follows:

$$b_i(\Gamma) = -0.00014\Gamma^2 + 0.027\Gamma - 0.322, \tag{1}$$

$$\mu_{m,i}(\Gamma) = -\ln(-0.000828\Gamma^2 + 0.0367\Gamma + 0.522), \tag{2}$$

$$\alpha_{m,i}(\Gamma, R) = \frac{EFD(\Gamma) p_e(R) p_l(\Gamma, R) p_p(R)}{\mu_{m,i} d_{ea}}, \tag{3}$$

where $EFD(\Gamma)$ is the total number of eggs laid by female mosquito per day, $p_e(R)$, $p_l(\Gamma, R)$ and $p_p(R)$ are the daily survival probabilities of eggs(e), larvae(l) and pupae(p), respectively, and d_{ea} is the time it takes an egg to develop to an adult.

The parameters $EFD(\Gamma)$,$p_e(R)$, $p_l(\Gamma, R)$, $p_p(R)$ and $d_{ea}(\Gamma)$ are given by:

$$EFD(\Gamma) = -0.153\Gamma^2 + 8.61\Gamma - 97.7, \tag{4}$$

$$p_i(R) = \frac{4p^*_i R(R_l - R)}{R_l^2}, i = e, l, p, \tag{5}$$

$$p_l(\Gamma, R) = e^{-(0.0554\Gamma - 0.06737)} \times p_l(R), \tag{6}$$

$$d_{ea}(\Gamma) = \frac{1}{-0.00094\Gamma^2 + 0.049\Gamma - 0.552}, \tag{7}$$

where p^*_i is the maximum daily survival probability of eggs, larvae and pupae, and R_l is the rainfall limit beyond which breeding sites get flushed out and no immature stages survive. $b_i(\Gamma)$, $\mu_{m,i}(\Gamma)$, $\alpha_{m,i}(\Gamma, R)$ and $\lambda_{m,i}(\Gamma)$ are positive, continuous, bounded and periodic functions of time t. For simplicity, the temperature and rainfall-dependent functions will be expressed as functions of t.

2.1. Mathematical model

The malaria transmission in each region $i = 1, ..., n$, can be described by the following non-autonomous metapopulation system with non-negative initial conditions:

$$\begin{aligned}
\frac{dS_{h,i}}{dt} &= \alpha_{h,i} + \phi_{h,i}T_{h,i} + \theta_{h,i}U_{h,i} - \left(p^{(h,i)}\lambda_{h,i} + \sum_{j=1}^{n} c_{j,i}^{S} + \mu_{h,i}\right) S_{h,i} + \sum_{j=1}^{n} c_{i,j}^{S} S_{h,j}, \\
\frac{dI_{h,i}}{dt} &= p^{(h,i)}\lambda_{h,i}S_{h,i} + \xi_{h,i}U_{h,i} - \left(d_{1,i} + \sum_{j=1}^{n} c_{j,i}^{I}\right) I_{h,i} + \sum_{j=1}^{n} c_{i,j}^{I} I_{h,j}, \\
\frac{dU_{h,i}}{dt} &= \eta_{h,i}I_{h,i} - \left(d_{2,i} + \sum_{j=1}^{n} c_{j,i}^{U}\right) U_{h,i} + \sum_{j=1}^{n} c_{i,j}^{U} U_{h,j}, \\
\frac{dT_{h,i}}{dt} &= \gamma_{h,i}I_{h,i} - \left(d_{3,i} + \sum_{j=1}^{n} c_{j,i}^{T}\right) T_{h,i} + \sum_{j=1}^{n} c_{i,j}^{T} T_{h,j}, \\
\frac{dS_{m,i}}{dt} &= \alpha_{m,i}(\Gamma, R)\left(1 - \frac{N_{m,i}}{K_i}\right) N_{m,i} - (p^{(m,i)}\lambda_{m,i} + \mu_{m,i}(\Gamma))S_{m,i}, \\
\frac{dI_{m,i}}{dt} &= p^{(m,i)}\lambda_{m,i}S_{m,i} - \mu_{m,i}(\Gamma)I_{m,i},
\end{aligned} \tag{8}$$

where the infection rates for humans ($\lambda_{h,i}$) and mosquitoes ($\lambda_{m,i}$) are given by

$$\lambda_{h,i} = \frac{a_i\beta_{h,i}}{N_{h,i}} I_{m,i}, \quad \lambda_{m,i}(\Gamma) = \frac{b_i(\Gamma)\beta_{m,i}}{N_{h,i}}(I_{h,i} + \pi_i U_{h,i}), \tag{9}$$

and

$$d_{1,i} = \eta_{h,i} + \gamma_{h,i} + \delta_{h,i} + \mu_{h,i}, \quad d_{2,i} = \xi_{h,i} + \theta_{h,i} + \mu_{h,i}, \quad d_{3,i} = \phi_{h,i} + \mu_{h,i}.$$

Hence, for region i, the human population $N_{h,i}(t)$, given by

$$N_{h,i}(t) = S_{h,i}(t) + I_{h,i}(t) + U_{h,i}(t) + T_{h,i}(t),$$

satisfies

$$\frac{dN_{h,i}(t)}{dt} = \alpha_{h,i} - \mu_{h,i}N_{h,i}(t) - \delta_{h,i}I_{h,i}(t) + \sum_{\Pi=S,I,U,T}\left(\sum_{j=1}^{n} c_{i,j}^{\Pi}\Pi_{h,j} - \sum_{j=1}^{n} c_{j,i}^{\Pi}\Pi_{h,i}\right). \tag{10}$$

The mosquito populations $N_{m,i}(t) = S_{h,i}(t) + I_{h,i}(t)$ satisfy

$$\begin{aligned}
\frac{dN_{m,i}(t)}{dt} &= \alpha_{m,i}(t)\left(1 - \frac{N_{m,i}(t)}{K_i}\right) N_{m,i}(t) - \mu_{m,i}(t)N_{m,i}(t), \\
&= \left(\alpha_{m,i}(t) - \mu_{m,i}(t)\right) N_{m,i}(t) - \frac{\alpha_{m,i}(t)}{K_i} N_{m,i}^2(t).
\end{aligned}$$

Table 1. Description of the state variables for system (8) in region $i = 1, ..., n$.

Variable	Description
$S_{h,i}$	Number of susceptible humans
$I_{h,i}$	Number of infectious humans
$U_{h,i}$	Number of effective antimalarial drug users
$T_{h,i}$	Number of counterfeit antimalarial drug users
$S_{m,i}$	Number of susceptible mosquitoes
$I_{m,i}$	Number of infectious mosquitoes

In the system (8) and equations (9), all constant parameters are positive except for the disease-induced death rates ($\delta_{h,i}$), which are assumed to be non-negative. The state variables and the parameters of the model are described in Tables 1 and 2. The table of parameters is given at a later point. The flow diagram of the model in one zone and the pattern of the human movement across the zones are illustrated in Figure 1 and Figure 2.

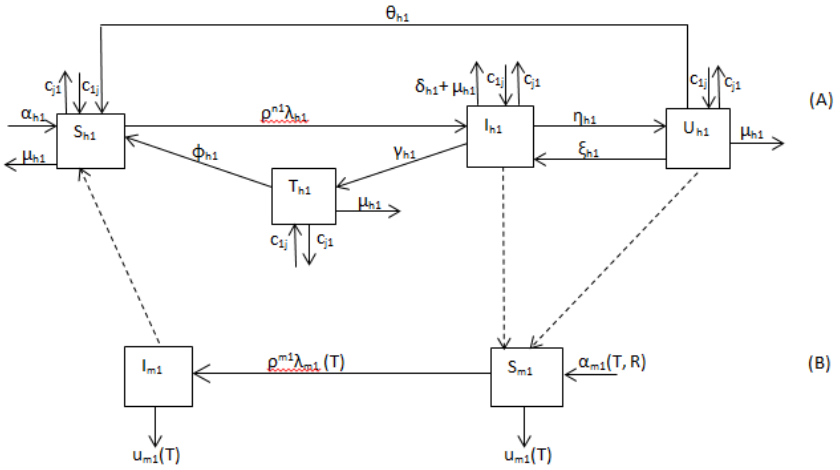

Figure 1. A flow diagram of malaria transmission within one zone: (A) Humans in zone 1 (B) Female anopheles mosquitoes in zone 1

3. Mathematical Analysis

The system (8) can be written as follows:

$$\dot{z}(t) = G(t, z(t)), \qquad z(0) > 0,$$

where

$$z = (z_j)_{1\leq j\leq 6n} = (Z_i)_{1\leq i\leq n} \quad \text{for} \quad Z_i = (S_{h,i}, I_{h,i}, U_{h,i}, T_{h,i}, S_{m,i}, I_{m,i})^T,$$

and $G : \mathbb{R}^1 \times \mathbb{R}^{6n}_+ \to \mathbb{R}^{6n}_+$ is defined by $G = (G_i)_{1\leq i\leq n}$, where

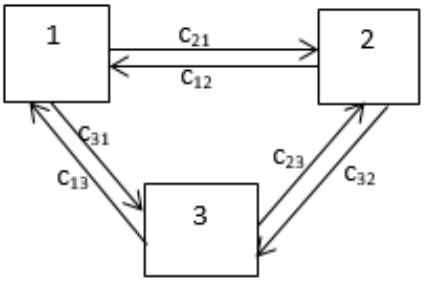

Figure 2. An illustration of human movement across zones (using three zones)

$$G_i(t,z) = \begin{pmatrix} \alpha_{h,i} + \phi_{h,i}T_{h,i} + \theta_{h,i}U_{h,i} - \left(p^{(h,i)}\lambda_{h,i} + \sum_{j=1}^{n} c_{j,i}^{S} + \mu_{h,i}\right) S_{h,i} + \sum_{j=1}^{n} c_{i,j}^{S} S_{h,j} \\ p^{(h,i)}\lambda_{h,i}S_{h,i} + \xi_{h,i}U_{h,i} - \left(d_{1,i} + \sum_{j=1}^{n} c_{j,i}^{I}\right) I_{h,i} + \sum_{j=1}^{n} c_{i,j}^{I} I_{h,j} \\ \eta_{h,i}I_{h,i} - \left(d_{2,i} + \sum_{j=1}^{n} c_{j,i}^{U}\right) U_{h,i} + \sum_{j=1}^{n} c_{i,j}^{U} U_{h,j} \\ \gamma_{h,i}I_{h,i} - \left(d_{3,i} + \sum_{j=1}^{n} c_{j,i}^{T}\right) T_{h,i} + \sum_{j=1}^{n} c_{i,j}^{T} T_{h,j} \\ \alpha_{m,i}(t)\left(1 - \frac{N_{m,i}}{K_i}\right) N_{m,i} - \left(p^{(m,i)}\lambda_{m,i}(t) + \mu_{m,i}(t)\right) S_{m,i} \\ p^{(m,i)}\lambda_{m,i}(t)S_{m,i} - \mu_{m,i}(t)I_{m,i} \end{pmatrix}, \tag{11}$$

for $1 \leq i \leq n$. We further introduce the notation $S_h = (S_{h,i})_{1\leq i\leq n}, I_h = (I_{h,i})_{1\leq i\leq n}, U_h = (U_{h,i})_{1\leq i\leq n}, T_h = (T_{h,i})_{1\leq i\leq n}, S_m = (S_{m,i})_{1\leq i\leq n}, I_m = (I_{m,i})_{1\leq i\leq n}$.

The following theorem establishes that system (8) is mathematically and epidemiologically well-posed.

Theorem 3.1. *For any initial value z in*

$$\begin{aligned} \Omega \;=\; & \{(S_h, I_h, U_h, T_h, S_m, I_m) \in \mathbb{R}_+^{6n} : 0 < S_{h,i} + I_{h,i} + U_{h,i} + T_{h,i}, \\ & 0 < S_{m,i} + I_{m,i}, i = 1, ..., n\}, \end{aligned}$$

system (8) has a unique nonnegative bounded solution through z for all $t \geq 0$.

Proof. Let $G(t,z)$ be the vector field defined in (11) with $z \in \Omega$. Then $G(t,z)$ is continuous and Lipschitzian in z on each compact subset of $\mathbb{R}_+^1 \times \Omega$. Clearly, $G(t,z) \geq 0$ whenever $z \geq 0$ and $z_k = 0, k = 1, ..., 6n$. It follows from Theorem 5.2.1 in [53] that there exists a unique nonnegative solution for the system (8) through $z \in \Omega$ in its maximal interval of existence.

The total numbers for humans and mosquitoes,

$$N_h(t) = \sum_{i=1}^{n} N_{h,i}(t) \text{ and } N_m(t) = \sum_{i=1}^{n} N_{m,i}(t),$$

satisfy

$$\frac{dN_h(t)}{dt} = \sum_{i=1}^{n}(\alpha_{h,i}-\mu_{h,i}N_{h,i}(t)-\delta_{h,i}I_{h,i})+\sum_{i=1}^{n}\left[\sum_{\Pi=S,I,U,T}\left(\sum_{j=1}^{n}c_{i,j}^{\Pi}\Pi_{h,j}-\sum_{j=1}^{n}c_{j,i}^{\Pi}\Pi_{h,i}\right)\right] \tag{12}$$

and

$$\frac{dN_m(t)}{dt} = \sum_{i=1}^{n}\alpha_{m,i}(t)\left(1-\frac{N_{m,i}(t)}{K_i}\right)N_{m,i}(t)-\sum_{i=1}^{n}\mu_{m,i}(t)N_{m,i}(t), \tag{13}$$

respectively.

Further computations of Eq. (12) show that the double summation gives zero and hence,

$$\frac{dN_h}{dt} \le \sum_{i=1}^{n}(\alpha_{h,i}-\mu_{h,i}N_{h,i}) \le \sum_{i=1}^{n}\alpha_{h,i}-\min_{1\le i\le n}\{\mu_{h,i}\}N_h, \tag{14}$$

and

$$\frac{dN_m(t)}{dt} \le r_mN_m(t)-\frac{\alpha_m}{K}\frac{(N_m(t))^2}{n} = \left(r_m-\frac{\alpha_m}{Kn}N_m(t)\right)N_m(t), \tag{15}$$

where

$$r_m = \max_{0\le t\le\omega}\left(\sum_{i=1}^{n}(\alpha_{m,i}(t)-\mu_{m,i}(t))\right) \quad \text{and} \quad \frac{\alpha_m}{K} = \min_{0\le t\le\omega}\left(\min_{1\le i\le n}\frac{\alpha_{m,i}(t)}{K_i}\right)$$

are positive constants.

Thus

$$N_h(t) \le \max\left[N_h(0), \frac{\sum_{i=1}^{n}\alpha_{h,i}}{\min\limits_{1\le i\le n}\{\mu_{h,i}\}}\right] \tag{16}$$

and

$$N_m(t) \le \max\left[N_m(0), \frac{nr_mK}{\alpha_m}\right].$$

By the comparison principle, we conclude that $N_m(t)$ is bounded as long as the solution exists. Hence, every solution of the system (8) exists globally. □

We assume $r_{m,i}(t) = \alpha_{m,i}(t)-\mu_{m,i}(t) > 0$ for $0 \le t \le \omega$.

Lemma 3.2. *The mosquito growth model Eq. (11) with $N_{m,i}(0) \ge 0$ for $i = 1, 2, ..., n$, has a unique positive periodic solution $N_m^*(t) \equiv (N_{m,1}^*(t), ..., N_{m,n}^*(t))$, which is globally asymptotically stable.*

Proof. The i^{th} equation of Eq. (11) is a Bernoulli equation whose solution (see Appendix for the calculations) is

$$N_{m,i}(t) = \frac{K_i N_{m,i}(0) e^{\int_0^t r_{m,i}(\tau)d\tau}}{N_{m,i}(0)\int_0^t \alpha_{m,i}(z) e^{\int_0^z r_{m,i}(\tau)d\tau} dz + K_i}. \tag{17}$$

The Poincaré map for this equation (assuming co-periodicity)

$$P(N_{m,i}(0)) = N_{m,i}(\omega) = \frac{K_i N_{m,i}(0) e^{\int_0^\omega r_{m,i}(\tau)d\tau}}{N_{m,i}(0)\int_0^w \alpha_{m,i}(z) e^{\int_0^z r_{m,i}(\tau)d\tau} dz + K_i}. \tag{18}$$

Fixed points follow immediately from the equation

$$N_{m,i}(0) = \frac{K_i N_{m,i}(0) e^{\int_0^\omega r_{m,i}(\tau)d\tau}}{N_{m,i}(0)\int_0^\omega \alpha_{m,i}(z) e^{\int_0^z r_{m,i}(\tau)d\tau} dz + K_i} \tag{19}$$

and they are $N_{m,i}(0) = 0$ or

$$N_{m,i}(0) = \frac{K_i(e^{\int_0^\omega r_{m,i}(\tau)d\tau} - 1)}{\int_0^\omega \alpha_{m,i}(z) e^{\int_0^z r_{m,i}(\tau)d\tau} dz} > 0, \tag{20}$$

if $r_{m,i}(\tau) > 0$.

Thus, using [55, Lemma 4.8], there is a unique nontrivial periodic solution to Eq. (11), namely the solution (17) originating from the initial condition (20). This solution is globally asymptotically stable. This follows from general theory as briefly described on [55, pp. 126-128]. Here we provide a direct proof, based on the observation on [55, p. 116] that the stability of the fixed point of the Poincaré map is equivalent to the stability of the periodic solution to (11). Thanks to the periodicity of the coefficients of the equation, the iterates of the Poincaré map are given as [55, p. 116],

$$P^{(k)}(N_{m,i}(0)) = \frac{K_i N_{m,i}(0) e^{\int_0^{k\omega} r_{m,i}(\tau)d\tau}}{N_{m,i}(0)\int_0^{k\omega} \alpha_{m,i}(z) e^{\int_0^z r_{m,i}(\tau)d\tau} dz + K_i}. \tag{21}$$

We have

$$e^{\int_0^{k\omega} r_{m,i}(\tau)d\tau} = \left(e^{\int_0^\omega r_{m,i}(\tau)d\tau}\right)^k =: \rho^k.$$

Further,

$$\int_0^{k\omega} \alpha_{m,i}(z) e^{\int_0^z r_{m,i}(\tau)d\tau} dz = \sum_{j=1}^{k} \int_{(j-1)\omega}^{j\omega} \alpha_{m,i}(z) e^{\int_0^z r_{m,i}(\tau)d\tau} dz$$

and, using the periodicity of $\alpha_{m,i}$ and $r_{m,i}$,

$$\int_{(j-1)\omega}^{j\omega} \alpha_{m,i}(z) e^{\int_0^z r_{m,i}(\tau)d\tau} dz = \int_{(j-1)\omega}^{j\omega} \alpha_{m,i}(z) e^{\int_0^{(j-1)\omega} r_{m,i}(\tau)d\tau} e^{\int_{(j-1)\omega}^z r_{m,i}(\tau)d\tau} dz$$
$$= \rho^{j-1} \int_{(j-1)\omega}^{j\omega} \alpha_{m,i}(z) e^{\int_{(j-1)\omega}^z r_{m,i}(\tau)d\tau} dz$$
$$= \rho^{j-1} \int_0^{\omega} \alpha_{m,i}(y+(j-1)\omega) e^{\int_{(j-1)\omega}^{y+(j-1)\omega} r_{m,i}(\tau)d\tau} dy$$
$$= \rho^{j-1} \int_0^{\omega} \alpha_{m,i}(y) e^{\int_0^y r_{m,i}(\sigma+(j-1)\omega)d\sigma} dy = \rho^{j-1} \int_0^{\omega} \alpha_{m,i}(y) e^{\int_0^y r_{m,i}(\sigma)d\sigma} dy =: \rho^{j-1} A_{m,i}.$$

Hence,

$$\int_0^{k\omega} \alpha_{m,i}(z) e^{\int_0^z r_{m,i}(\tau)d\tau} dz = \sum_{j=1}^{k} \rho^{j-1} A_{m,i} = \frac{\rho^k - 1}{\rho - 1} A_{m,i}, \quad \rho > 1.$$

Thus

$$\lim_{k\to\infty} P^{(k)}(N_{m,i}(0)) = \lim_{k\to\infty} \frac{K_i N_{m,i}(0) \rho^k}{N_{m,i}(0) \frac{\rho^k - 1}{\rho - 1} A_{m,i} + K_i} = \frac{K_i(\rho - 1)}{A_{m,i}},$$

which agrees with (20).

Next, we find the periodic solution explicitly. The solution (17) with $N_{m,i}(0)$ given by (20) can be written as

$$N_{m,i}(t) = \frac{K_i(\rho - 1) e^{\int_0^t r_{m,i}(\tau)d\tau}}{(\rho - 1) \int_0^t \alpha_{m,i}(z) e^{\int_0^z r_{m,i}(\tau)d\tau} dz + A_{m,i}}.$$

Let $t = k\omega + t'$ for $t' \in [0, \omega)$. Then, similarly to the above,

$$e^{\int_0^t r_{m,i}(\tau)d\tau} = \rho^k e^{\int_0^{t'} r_{m,i}(\tau)d\tau}$$

and

$$\int_0^t \alpha_{m,i}(z) e^{\int_0^z r_{m,i}(\tau)d\tau} dz = \int_0^{k\omega} \alpha_{m,i}(z) e^{\int_0^z r_{m,i}(\tau)d\tau} dz + \int_{k\omega}^{k\omega+t'} \alpha_{m,i}(z) e^{\int_0^z r_{m,i}(\tau)d\tau} dz$$
$$= A_{m,i} \frac{\rho^k - 1}{\rho - 1} + \rho^k \int_0^{t'} \alpha_{m,i}(z) e^{\int_0^z r_{m,i}(\tau)d\tau} dz.$$

Hence, for $t \in [k\omega, (k+1)\omega)$, we have

$$\begin{aligned} N_{m,i}(t) &= \frac{K_i(\rho-1)\rho^k e^{\int_0^{t'} r_{m,i}(\tau)d\tau}}{A_{m,i}(\rho^k-1)+(\rho-1)\rho^k\int_0^{t'}\alpha_{m,i}(z)e^{\int_0^z r_{m,i}(\tau)d\tau}dz + A_{m,i}} \\ &= \frac{K_i(\rho-1)e^{\int_0^{t'} r_{m,i}(\tau)d\tau}}{A_{m,i}+(\rho-1)\int_0^{t'}\alpha_{m,i}(z)e^{\int_0^z r_{m,i}(\tau)d\tau}dz} \\ &= \frac{K_i(e^{\int_0^{\omega} r_{m,i}(\tau)d\tau}-1)e^{\int_0^{t'} r_{m,i}(\tau)d\tau}}{\int_0^{\omega}\alpha_{m,i}(z)e^{\int_0^z r_{m,i}(\sigma)d\sigma}dz + (e^{\int_0^{\omega} r_{m,i}(\tau)d\tau}-1)\int_0^{t'}\alpha_{m,i}(z)e^{\int_0^z r_{m,i}(\tau)d\tau}dz}. \end{aligned}$$

□

We now show the existence of a unique disease-free solution and then evaluate the reproduction ratio for the system.

4. Disease-free equilibrium and reproduction ratio

4.1. Disease-free equilibrium

A disease-free equilibrium is an equilibrium solution of the system (8) where no disease exists in any of the regions. To obtain the disease-free periodic solutions

$$E_0^+ = (S^*_{h,1}, ..., S^*_{h,n}, 0, ..., 0, 0, ..., 0, 0, ..., 0, S^*_{m,1}(t), ..., S^*_{m,n}(t), 0, ..., 0),$$

we decouple the system (8) into the human metapopulation model and the mosquito periodic model to give

$$\frac{dS_{h,i}}{dt} = \alpha_{h,i} - \left(\sum_{j=1}^{n} c^S_{j,i} + \mu_{h,i}\right) S_{h,i} + \sum_{j=1}^{n} c^S_{i,j} S_{h,j}, \quad 1 \le i \le n, \tag{22}$$

and

$$\frac{dS_{m,i}}{dt} = \alpha_{m,i}(t)\left(1 - \frac{S_{m,i}}{K_i}\right) S_{m,i} - \mu_{m,i}(t) S_{m,i}, \quad 1 \le i \le n. \tag{23}$$

Denote $S^*_h = (S^*_{h,1}, S^*_{h,2}, ..., S^*_{h,n})^T$, $\alpha_h = (\alpha_{h,1}, \alpha_{h,2}, ..., \alpha_{h,n})^T$, $M_h = diag(\mu_{h,1} + \sum_{j=1}^n c^S_{j1}) - C^S$, $1 \le i \le n$, and $S^*_m = (S^*_{m,1}, S^*_{m,2}, ..., S^*_{m,n})^T$.

Lemma 4.1. *The system (8) has a unique disease free equilibrium solution E_0^+.*

Proof. Setting Eq. (22) equal to zero yields the algebraic system

$$\alpha_{h,i} - \left(\sum_{j=1}^{n} c^S_{j,i} + \mu_{h,i}\right) S_{h,i} + \sum_{j=1}^{n} c^S_{i,j} S_{h,j} = 0, \quad 1 \le i \le n, \tag{24}$$

or, in matrix form,

$$\alpha_h - M_h S_h^* = 0, \tag{25}$$

where $M_h = diag\left(\sum_{j=1}^{n} c_{j,i}^S + \mu_{h,i}\right) - C^S, \quad 1 \leq i \leq n.$

In order to solve Eq. (25), we recall that C^S is assumed to be irreducible, and this ensures that M_h is also irreducible. We note that since M_h has negative off-diagonal entries and positive column sums, M_h is a non-singular M-matrix. Then, since $\alpha_h > 0$ and $M_h^{-1} > 0$, we have that the system Eq. (25) has a unique positive solution given by $S_h^* = M_h^{-1}\alpha_h > 0$. Eq. (23) first gives a trivial equilibrium solution $S_{m,i}(t) = 0$. For nontrivial solutions, we observe that Eq. (23) is the same as Eq. (11), and thus, the existence of a unique nontrivial periodic solution follows as in Lemma 3.2. So there exists a unique disease free equilibrium solution E_0^+ for the system (8). □

4.2. Reproduction ratio

The reproduction ratio is the expected number of secondary cases produced by an infective (either infectious or counterfeit drug user) individual introduced into a homogeneous, completely susceptible population. The reproduction ratio is a threshold parameter, usually linked to the stability of the disease-free equilibrium. Several methods are used to calculate R_0 for periodic systems, [59]. We establish the reproduction ratio for the metapopulation malaria transmission model based on the theory developed in [48], which generalises the approach in [47] to periodic models.

Linearizing system (8) at E_0^+, we obtain the following system for the "infected or diseased" classes:

$$\begin{aligned}
\frac{dI_{h,i}}{dt} &= p^{(h,i)} a_i \beta_{h,i} I_{m,i} + \xi_{h,i} U_{h,i} - (d_{1,i} + \sum_{j=1}^{n} c_{ji}^I) I_{h,i} + \sum_{j=1}^{n} c_{ij}^I I_{h,j}, \\
\frac{dU_{h,i}}{dt} &= \eta_{h,i} I_{h,i} - (d_{2,i} + \sum_{j=1}^{n} c_{ji}^U) U_{h,i} + \sum_{j=1}^{n} c_{ij}^U U_{h,j}, \\
\frac{dI_{m,i}}{dt} &= p^{(m,i)} b_i(t) \beta_{m,i} \frac{S_{m,i}^*}{N_{h,i}^*} (I_{h,i} + \pi_i U_{h,i}) - \mu_{m,i}(t) I_{m,i},
\end{aligned} \tag{26}$$

where $i = 1, ..., n$.

Let $X = (I_h, U_h, I_m)$. The subsystem (26) can be rewritten as: $\dot{X} = (F(t) - V(t))X$, where F and V are $3n \times 3n$ matrices that are given by $F(t) = diag(F_{ii}(t)), i = 1, .., n$, where

$$F_{ii}(t) = \begin{pmatrix} 0 & 0 & p^{(h,i)} a_i \beta_{h,i} \\ 0 & 0 & 0 \\ p^{(m,i)} b_i(t) \beta_{m,i} \frac{S_{m,i}^*}{N_{h,i}^*} & p^{(m,i)} b_i(t) \beta_{m,i} \pi_i \frac{S_{m,i}^*}{N_{h,i}^*} & 0 \end{pmatrix}, \tag{27}$$

and $V(t) = (V_{ij}(t))_{1\leq i,j\leq n}$, with $V_{ij} = diag(-c_{ij}^I, -c_{ij}^U, 0)$, $i \neq j$, and

$$V_{ii}(t) = \begin{pmatrix} d_{1,i} + \sum_{j=1}^n c_{ji}^I & -\xi_{h,i} & 0 \\ -\eta_{h,i} & d_{2,i} + \sum_{j=1}^n c_{ji}^U & 0 \\ 0 & 0 & \mu_{m,i}(t) \end{pmatrix}, \tag{28}$$

where

$$d_{1,i} = \eta_{h,i} + \gamma_{h,i} + \delta_{h,i} + \mu_{h,i} \quad \text{and} \quad d_{2,i} = \xi_{h,i} + \theta_{h,i} + \mu_{h,i}.$$

Let $Y(t,s)$, $t \geq s$, be the evolution operator of the linear ω-periodic system

$$\frac{dy}{dt} = -V(t)y, \tag{29}$$

that is, for each $s \in \mathbb{R}^1$, the $3n \times 3n$ matrix $Y(t,s)$ satisfies

$$\frac{dY(t,s)}{dt} = -V(t)Y(t,s), \quad \forall \quad t \geq s, \quad Y(s,s) = I_{3n}, \tag{30}$$

where I_{3n} is the $3n \times 3n$ identity matrix.

Let C_ω be the ordered Banach space of all ω-periodic functions from $\mathbb{R}^1$ to $\mathbb{R}^{3n}$ equipped with the maximum norm $\| \ . \ \|$ and the positive cone $C_\omega^+ := \{\phi \in C_\omega : \phi(t) \geq 0, \forall t \in \mathbb{R}\}$. For the periodic environment, the distribution of the infectious individuals is considered to be $\phi(s) \in C_\omega$ at $t = 0$, so that the distribution of new infections produced by the infected individuals, who were introduced at time s is given by $F(s)\phi(s)$ and $Y(t,s)F(s)\phi(s)$ represents the distribution of those infected individuals, who were newly infected at time s and remain in the infective class at time t for $t \geq s$. It follows that

$$(\psi)(t) = \int_{-\infty}^t Y(t,s)F(s)\phi(s)ds \tag{31}$$

$$= \int_0^\infty Y(t,t-a)F(t-a)\phi(t-a)da, \quad \forall t \in \mathbb{R}^1, \quad \phi \in C_\omega, \tag{32}$$

is the distribution of new infections at time t produced by all those infected individuals $\phi(s)$ introduced at previous time to t.

Let $L : C_\omega \to C_\omega$ be defined by

$$(L\phi)(t) = \int_0^\infty Y(t,t-a)F(t-a)\phi(t-a)da, \quad \forall t \in \mathbb{R}^1, \quad \phi \in C_\omega. \tag{33}$$

It is easy to verify that conditions $(A1)$-$(A7)$ in [48] are satisfied. Then, L is the next infection operator, and the reproduction ratio of the system (8) is defined as $R_0 := \rho(L)$, the spectral radius of L.

Thus,

$$R_0 := \rho(L) = \rho\bigg(\int_0^\infty Y(t,t-a)F(t-a)\phi(t-a)da\bigg). \tag{34}$$

In order to calculate R_0, we let $W(t,s,\lambda)$, $t \geq s$, $s \in \mathbb{R}$, be the evolution operator of the linear periodic system

$$\dot{W} = \left[\frac{F(t)}{\lambda} - V(t)\right]W, \quad \forall t \in \mathbb{R}. \tag{35}$$

It is clear that $W(t,0,1) = \Phi_{F-V}(t), \forall t \geq 0$ (Theorem 2.1 in [48]).

The following lemma shows that the reproduction ratio R_0 is the threshold parameter for the local stability of the disease-free periodic solution.

Lemma 4.2. *(Theorem 2.2 in [48]). Let $\Phi_{F-V}(t)$ and $\rho(\Phi_{F-V}(\omega))$ be the monodromy matrix of system (8) and the spectral radius of $\Phi_{F-V}(\omega)$, respectively. The following statements are valid:*

(i) $R_0 = 1$ *if and only if* $\rho(\Phi_{F-V}(\omega)) = 1$.
(ii) $R_0 > 1$ *if and only if* $\rho(\Phi_{F-V}(\omega)) > 1$.
(iii) $R_0 < 1$ *if and only if* $\rho(\Phi_{F-V}(\omega)) < 1$.

Theorem 4.3. *The disease-free periodic solution E_0^+ of the system (8) is stable if $R_0 < 1$ and unstable if $R_0 > 1$.*

Proof. Let $\zeta(t)$ be the Jacobian matrix for the system (8) evaluated at the disease-free periodic solution. Then, we have

$$\zeta(t) \;=\; \begin{pmatrix} F(t) - V(t) & 0 \\ \zeta_{21}(t) & \zeta_{22}(t) \end{pmatrix}, \tag{36}$$

where matrices $\zeta_{11}(t)$ and $\zeta_{12}(t)$ can be written as

$$\zeta_{22}(t) = \begin{pmatrix} -M_h & 0 & 0 \\ 0 & 0 & 0 \\ 0 & 0 & -M_m(t) \end{pmatrix},$$

and

$$\zeta_{21}(t) = \begin{pmatrix} 0 & 0 & -p^{(h,i)}a_i\beta_{h,i} \\ 0 & 0 & 0 \\ -p^{(m,i)}b_i(t)\beta_{m,i}\frac{S^*_{m,i}}{N^*_{h,i}} & -p^{(m,i)}b_i(t)\beta_{m,i}\pi_i\frac{S^*_{m,i}}{N^*_{h,i}} & 0 \end{pmatrix}, \tag{37}$$

where $M_m(t) = diag(\mu_{m,i}(t))$, $i = 1, ..., n$.

The matrix $\zeta(t)$ is a triangular matrix, and therefore the disease-free equilibrium is locally asymptotically stable if $\rho(\Phi_{\zeta_{22}}(\omega)) < 1$ and $\rho(\Phi_{F-V}(\omega)) < 1$. We note that, the matrix ζ_{22} has eigenvalues with negative real parts (since the matrices M_h and M_m are nonsingular M-matrices, see, for instance [57]). It then follows that $\rho(\Phi_{\zeta_{22}}(\omega)) < 1$. Therefore, the stability of the disease-free periodic solution depends on $\rho(\Phi_{F-V}(\omega))$. If $\rho(\Phi_{F-V}(\omega)) < 1$, then E_0^+ is stable and if $\rho(\Phi_{F-V}(\omega)) > 1$, then E_0^+ is unstable. By Lemma Eq 4.2 (Theorem 2.2 in [48]), $\rho(\Phi_{F-V}(\omega)) < 1 (> 1)$ is equivalent to $R_0 < 1 (> 1)$. Hence, E_0^+ is stable when $R_0 < 1$ and unstable when $R_0 > 1$. □

5. Case study: three ecological zones of Ghana

This section looks at malaria transmission across three zones (i.e. $n = 3$). Ghana is a country which lies on the south-central coast of West Africa and shares a common border in the east, north and west with the Republics of Togo, Burkina Faso and Cote d'Ivoire, respectively, with the Gulf of Guinea and the Atlantic Ocean to the south [61]. The three ecological zones of Ghana are the Northern Savannah, the Forest Zone and the Coastal Savannah Zone [20]. Tamale, Kumasi and Accra are the largest cities within the Northern Savannah zone, the Forest zone and the Coastal Savannah, respectively, which are interconnected by travel [60]. Accra is also the capital of Ghana. Figure 3 shows a map of the three ecological zones.

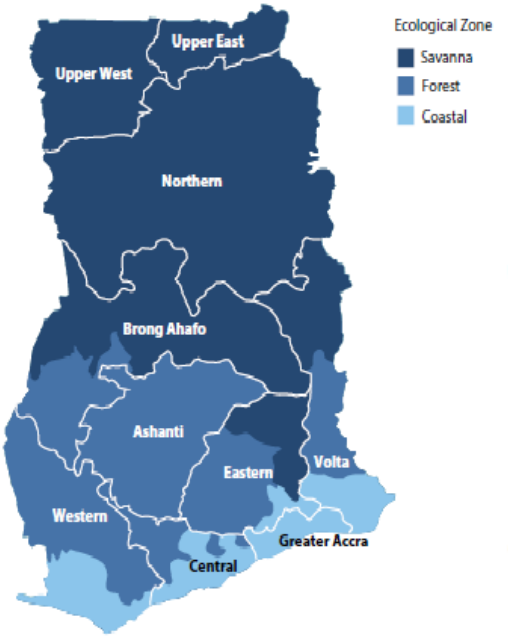

Figure 3. A map of illustrating the three ecological zones and the 10 regions of Ghana. Source: [20]

The Northern savannah zone has short trees or a continuous grass cover interspersed with generally fire-resistant, deciduous, broad-leaf trees, shorter grasses and shrubs. The forest zone has forest reserves and farmlands with an even tree canopy at $30 - 60$ meters, which may be deciduous in the dry season, but the understorey shrubs and trees are evergreen. The coastal savannah is low-lying, with mainly grass and shrubs. This zone occurs along the coastline, around lagoons and estuaries of the larger rivers. The vegetation is mainly grass and scrub [63, 64].

Rainfall distribution for Ghana is bimodal in the forest and coastal zones, i.e., March to July and September to October and unimodal in the northern savannah zone, i.e. May to October. The average monthly rainfall and high-temperature values for Accra, Kumasi and Tamale are given in Table 3.

5.1. Malaria in Ghana

Ghana is a malaria-endemic country, and in 2020, Ghana was among the 29 out of the 85 malaria-endemic countries that accounted for 96% of malaria cases and deaths globally [2, 3]. The main parasite species responsible for malaria in Ghana is *P. falciparum*, while *Anopheles gambiae s.c.* and *A. funestus* are major vectors found throughout the country [15, 26, 27]. Malaria transmission varies across the country, with the intensity of approximately $6-7$ months (May-October) in the northern savannah and up to $10-11$ months in the forest zone [20, 61].

5.2. Parameter estimation

The numerical simulations of the climate-based metapopulation model are done using MATLAB software ode45 and CFTOOL. Tamale is chosen as Zone 1, while Kumasi and Accra are taken as Zones 2 and 3, respectively. The total human populations of Tamale ($N_{h,1}$), Kumasi ($N_{h,2}$) and Accra ($N_{h,3}$) are estimated to be $360,579$, $1,468,609$ and $1,963,264$, respectively [60]. It follows that, at the disease-free steady-state, $\alpha_{h,1}/\mu_{h,1} = 360,579$, $\alpha_{h,2}/\mu_{h,2} = 1,468,609$ and $\alpha_{h,3}/\mu_{h,3} = 1,963,264$. The life expectancy is 67.4 years for Ghana [68]. Therefore, the natural death rate is given by $\mu_{h,i} = \frac{1}{67.4*12} = 1.236399604 \times 10^{-3}[month^{-1}]$, and the birth rates are given by $\alpha_{h,1} = 455.7704$, $\alpha_{h,2} = 1856.3160$ and $\alpha_{h,3} = 2481.5579$ per month. Data on the number of malaria outpatient cases, inpatient cases, patients who received the effective antimalarial drug (ACTs) treatment, deaths and malaria parasitaemia prevalence for the various regions and zones for 2016 are taken from [62, 69]. For the travel rates, we assume that more people travel to Accra (Zone 3) for official businesses, services, trading (imports and exports), urbanization and international travel. This is followed by Kumasi, which is usually a middle ground for trading farm products from the northern part of the country and importing goods from the southern part of the country. Hence, we set: $c_{12}^{\Pi} = 0.3, c_{13}^{\Pi} = 0.2, c_{21}^{\Pi} = 0.5, c_{23}^{\Pi} = 0.5, c_{31}^{\Pi} = 0.3, c_{31}^{\Pi} = 0.9$, for $\Pi = S, I, U, T$.

Unless otherwise stated, we use the values listed in Table 2 for constant parameters in the simulation. The periodic parameters are evaluated using the monthly mean high temperatures and the rainfall of the three cities obtained from Weather Atlas websites, [65, 67] and [66], as shown in Table 3. Climate data is the weather statistics, usually over a 30-year interval (https://www.weather-atlas.com/en/ghana-climate).

Using CFTOOL in Matlab, the temperature (Γ) dependent mosquito biting rate ($b_i(\Gamma)$ in Equation 2) for Tamale, Kumasi and Accra can be fitted by

$$\begin{aligned} b_1(t) &= 0.4214 + 0.03395\cos(\pi t/6) + 0.05531\sin(\pi t/6) - 0.0003732\cos(2\pi t/6) \\ &- 0.01332\sin(2\pi t/6) - 0.002604\cos(3\pi t/6) - 0.008566\sin(3\pi t/6) \\ &- 0.001174\cos(4\pi t/6) - 0.007401\sin(4\pi t/6) + 0.004061\cos(5\pi t/6) \\ &- 0.001354\sin(5\pi t/6)[month^{-1}], \end{aligned}$$

$$\begin{aligned} b_2(t) &= 0.3736 + 0.01986\cos(\pi t/6) + 0.04003\sin(\pi t/6) - 0.006129\cos(2\pi t/6) \\ &- 0.0105\sin(2\pi t/6) - 0.007431\cos(3\pi t/6) - 0.0002601\sin(3\pi t/6) \\ &- 0.003688\cos(4\pi t/6) - 0.003466\sin(4\pi t/6)[month^{-1}], \end{aligned}$$

Table 2. Description of the parameters for the model in (8) and their values for Tamale(1), Kumasi(2) and Accra(3)

Parameter	Description	Value for zone 1,2&3	Unit	Reference
$\alpha_{h,i}$	The birth rate of humans	14.657,59.697,79.804	$month^{-1}$	Estimated
$\alpha_{m,i}$	The recruitment rate of adult mosquitoes	in the text		
$\beta_{h,i}$	The transmission probability from infectious mosquitoes to humans	0.025/[0.007-0.04],0.07/[0.04-0.102],0.02	dimensionless	[15, 26, 27]
$\beta_{m,i}$	The transmission probability from infected humans to mosquitoes	0.5,0.2,0.2	dimensionless	Assumed
π_i	The degree of infectiousness of counterfeit drug users	0.5	dimensionless	Assumed
a_i	The average number of mosquito bites per human	990,150,330/[30-1020]	$month^{-1}$	[15, 26, 27]
b_i	The per capita biting rate of mosquitoes	in the text		
$n_{h,i}$	The average disease latent period in humans	$0.4/[0.3 - 0.57]$	$month^{-1}$	[40]
$p^{(h,i)}$	The probability of surviving the average latent period in humans	to be evaluated	dimensionless	
$\eta_{h,i}$	The per capita rate of infectious humans becoming counterfeit drug users	[1-4.3]	$month^{-1}$	[49]
$\gamma_{h,i}$	The per capita rate of infectious humans becoming fully cured	[1-10]	$month^{-1}$	[49]
$\xi_{h,i}$	The per capita rate of recrudescence	[1-4.3]	$month^{-1}$	[49]
$\phi_{h,i}$	The per capita rate of the loss of post-treatment prophylaxis	0.167/[0.042-2.143]	$month^{-1}$	[49]
$\theta_{h,i}$	The per capita rate of semi-immune counterfeit drug users becoming susceptible	0.0833	$month^{-1}$	Assumed
$\mu_{h,i}$	The natural death rate of humans	4.0649×10^{-5}	$month^{-1}$	[68]
$\delta_{h,i}$	The per capita disease-induced death rate of humans	0.0047,0.00168,0.00584	$month^{-1}$	[62]
$n_{m,i}$	The average disease latent period in mosquitoes	0.367	$month^{-1}$	[40]
$p^{(m,i)}$	The probability of surviving the average latent period in mosquitoes	to be evaluated	dimensionless	
$\mu_{m,i}$	The per capita death rate of mosquitoes	in the text		
p_e^*	The maximum daily survival probability of eggs	0.9	dimensionless	[70]
p_l^*	The maximum daily survival probability of larvae	0.25	dimensionless	[70]
p_p^*	The maximum daily survival probability of pupae	0.75	dimensionless	[70]
R_l	The rainfall limit beyond which breeding sites are flushed out, and no immature stages survive	300,230,210	dimensionless	Assumed

Table 3. Monthly mean high temperatures (in ^oC) and the rainfalls (in mm) for the three cities- Tamale, Kumasi and Accra within the Northern Savannah, Forest and Coastal Savannah ecological zones of Ghana. Source: [65, 67] and [66].

Zone(City)	Climate	Jan.	Feb.	Mar.	Apr.	May	June	July	Aug.	Sept.	Oct.	Nov.	Dec.
N.Savannah	Temp.	35	37	37	35	34	31	30	29	30	32	35	35
(Tamale)	Rain.	5	13	48	89	112	145	142	198	231	91	15	3
Forest	Temp.	31.9	33.5	32.9	32.3	31.3	29.5	28	27.7	28.7	30.1	31.2	30.7
(Kumasi)	Rain.	15.1	66.3	137	129.3	174.4	214.3	157.5	89.9	165.2	153.3	74.3	25.8
C.Savannah	Temp.	31	31	31	31	31	29	27	27	27	29	31	31
(Accra)	Rain.	15	33	56	81	142	178	46	15	36	64	36	23

and

$$\begin{aligned} b_3(t) &= 0.3525 + 0.001575\cos(\pi t/6) + 0.04288\sin(\pi t/6) + 0.0153\cos(2\pi t/6) \\ &- 0.001182\sin(2\pi t/6) + 0.0003305\cos(3\pi t/6) + 0.003835\sin(3\pi t/6) \\ &+ 0.005862\cos(4\pi t/6) - 0.001157\sin(4\pi t/6)[month^{-1}], \end{aligned}$$

respectively.

The discrete data and the corresponding fitted curves for $b_1(t)$, $b_2(t)$ and $b_3(t)$ are shown in Figure 4. The temperature-dependent death rate of the mosquitoes (in Eq. 2)

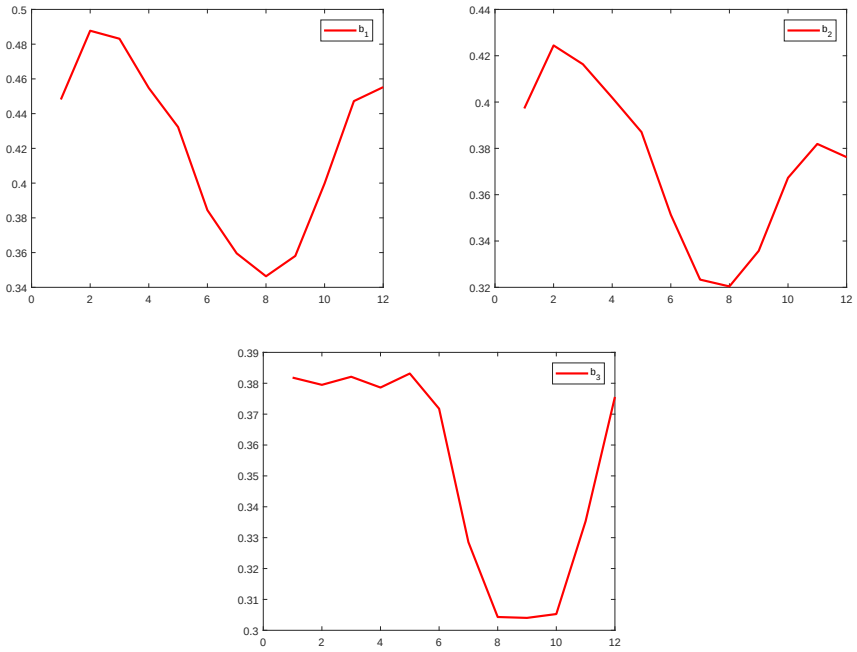

Figure 4. Fitting curves for $b_1(t)$, $b_2(t)$ and $b_3(t)$

for Tamale, Kumasi and Accra can be approximated by

$$\begin{aligned}\mu_{m,1}(t) &= 0.201 + 0.04107\cos(\pi t/6) + 0.06943\sin(\pi t/6) - 0.007137\cos(2\pi t/6)\\ &- 0.009306\sin(2\pi t/6) - 0.002831\cos(3\pi t/6) - 0.01414\sin(3\pi t/6)\\ &+ 0.000177\cos(4\pi t/6) - 0.01288\sin(4\pi t/6) + 0.005153\cos(5\pi t/6)\\ &- 0.001622\sin(5\pi t/6)[month^{-1}],\end{aligned}$$

$$\begin{aligned}\mu_{m,2}(t) &= 0.1439 + 0.01568\cos(\pi t/6) + 0.03564\sin(\pi t/6) - 0.007754\cos(2\pi t/6)\\ &- 0.005524\sin(2\pi t/6) - 0.006285\cos(3\pi t/6) - 0.001734\sin(3\pi t/6)\\ &- 0.004006\cos(4\pi t/6) - 0.004233\sin(4\pi t/6) - 0.0003993\cos(5\pi t/6)\\ &- 0.002556\sin(5\pi t/6)[month^{-1}],\end{aligned}$$

and

$$\begin{aligned}\mu_{m,3}(t) &= 0.1271 + 0.005604\cos(\pi t/6) + 0.02871\sin(\pi t/6) + 0.009537\cos(2\pi t/6)\\ &- 0.003849\sin(2\pi t/6) + 0.001899\cos(3\pi t/6) + 0.002877\sin(3\pi t/6)\\ &+ 0.003297\cos(4\pi t/6) - 0.003092\sin(4\pi t/6)[month^{-1}],\end{aligned}$$

respectively.

The discrete data and the corresponding fitted curves for $\mu_{m1}(t)$, $\mu_{m2}(t)$ and $\mu_{m3}(t)$, $i = 1, 2, 3$ are shown in Figure 5.

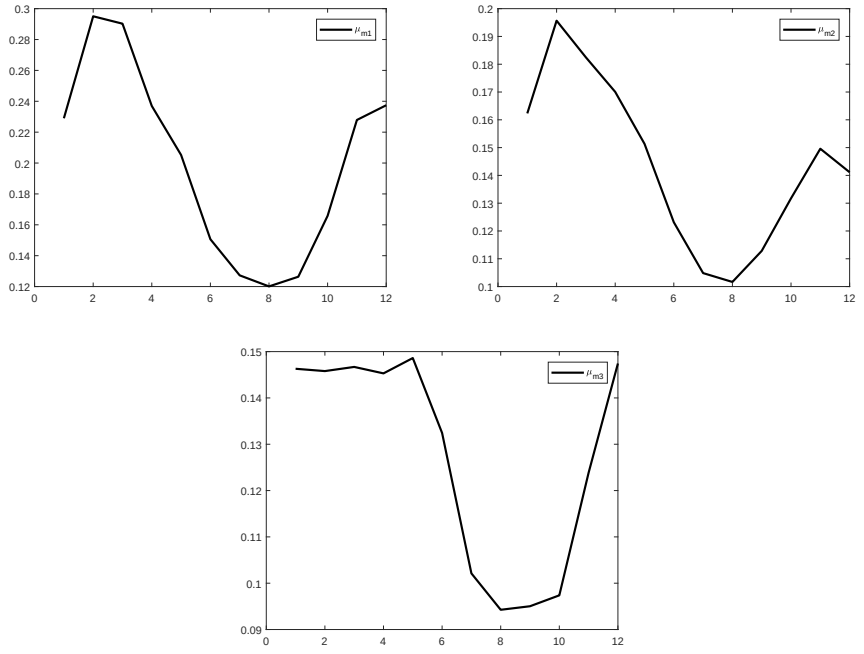

Figure 5. Fitting curves for $\mu_{m1}(t)$, $\mu_{m2}(t)$ and $\mu_{m3}(t)$

Lastly, the temperature-rainfall dependent adult mosquito recruitment rate (given

in Eq. 3) for Tamale, Kumasi and Accra can also be fitted by

$$\begin{aligned}\alpha_{m,1}(t) &= 0.1741 - 0.1987\cos(\pi t/6) - 0.1762\sin(\pi t/6) + 0.02554\cos((2\pi t/6)\\ &+ 0.1116\sin(2\pi t/6) - 0.005287\cos(3\pi t/6) - 0.04392\sin(3\pi t/6)\\ &- 0.01632\cos(4\pi t/6) + 0.02141\sin(4\pi t/6) - 0.01053\cos(5\pi t/6)\\ &+ 0.02422\sin(5\pi t/6)[month^{-1}],\end{aligned}$$

$$\begin{aligned}\alpha_{m,2}(t) &= 0.2704 - 0.1128\cos(\pi t/6) - 0.2181\sin(\pi t/6) - 0.1422\cos(2\pi t/6)\\ &+ 0.05884\sin(2\pi t/6) + 0.1031\cos(3\pi t/6) - 0.07885\sin(3\pi t/6)\\ &- 0.1069\cos(4\pi t/6) - 0.01394\sin(4\pi t/6) + 0.01938\cos(5\pi t/6)\\ &+ 0.02929\sin(5\pi t/6)[month^{-1}],\end{aligned}$$

and

$$\begin{aligned}\alpha_{m,3}(t) &= 0.1795 - 0.08071\cos(\pi t/6) - 0.01276\sin(\pi t/6) - 0.06008\cos(2\pi t/6)\\ &- 0.1101\sin(2\pi t/6) - 0.03284\cos(3\pi t/6) - 0.02312\sin(3\pi t/6)\\ &- 0.04918\cos(4\pi t/6) + 0.10144\sin(4\pi t/6) + 0.07608\cos(5\pi t/6)\\ &- 0.0009537\sin(5\pi t/6)[month^{-1}].\end{aligned}$$

The discrete data and the corresponding fitted curves for $\alpha_{m1}(t)$, $\alpha_{m2}(t)$ and $\alpha_{m3}(t)$ are shown in Figure 6. The matrices F and V in this case are

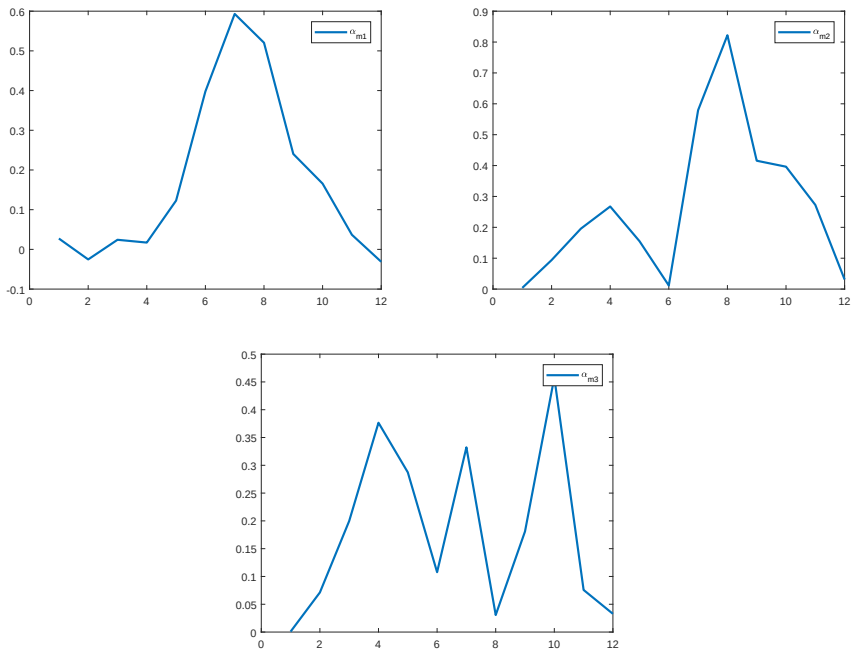

Figure 6. Fitting curves for $\alpha_{m1}(t)$, $\alpha_{m2}(t)$ and $\alpha_{m3}(t)$

$$F = \begin{pmatrix} 0 & 0 & 0 & 0 & 0 & 0 & f_4 & 0 & 0 \\ 0 & 0 & 0 & 0 & 0 & 0 & 0 & f_5 & 0 \\ 0 & 0 & 0 & 0 & 0 & 0 & 0 & 0 & f_6 \\ 0 & 0 & 0 & 0 & 0 & 0 & 0 & 0 & 0 \\ 0 & 0 & 0 & 0 & 0 & 0 & 0 & 0 & 0 \\ 0 & 0 & 0 & 0 & 0 & 0 & 0 & 0 & 0 \\ f_1 & 0 & 0 & \pi_1 f_1 & 0 & 0 & 0 & 0 & 0 \\ 0 & f_2 & 0 & 0 & \pi_2 f_2 & 0 & 0 & 0 & 0 \\ 0 & 0 & f_3 & 0 & 0 & \pi_3 f_3 & 0 & 0 & 0 \end{pmatrix},$$

and

$$V = \begin{pmatrix} v_1 & -c_{12}^I & -c_{13}^I & -\xi_{h,1} & 0 & 0 & 0 & 0 & 0 \\ -c_{21}^I & v_2 & -c_{23}^I & 0 & -\xi_{h,2} & 0 & 0 & 0 & 0 \\ -c_{31}^I & -c_{32}^I & v_3 & 0 & 0 & -\xi_{h,3} & 0 & 0 & 0 \\ -\eta_{h,1} & 0 & 0 & v_4 & -c_{12}^U & -c_{13}^U & 0 & 0 & 0 \\ 0 & -\eta_{h,2} & 0 & -c_{21}^U & v_5 & -c_{23}^U & 0 & 0 & 0 \\ 0 & 0 & -\eta_{h,3} & -c_{31}^U & -c_{32}^U & v_6 & 0 & 0 & 0 \\ 0 & 0 & 0 & 0 & 0 & 0 & \mu_{m,1} & 0 & 0 \\ 0 & 0 & 0 & 0 & 0 & 0 & 0 & \mu_{m,2} & 0 \\ 0 & 0 & 0 & 0 & 0 & 0 & 0 & 0 & \mu_{m,3} \end{pmatrix},$$

where $f_1, ..., f_6$ and $v_1, ..., v_6$ are defined by

$$f_1 = p^{(m,1)} b_1(t) \beta_{m,1} \frac{S_{m,1}^*}{S_{h,1}^*}, \quad f_2 = p^{(m,2)} b_2(t) \beta_{m,2} \frac{S_{m,2}^*}{S_{h,2}^*}, \quad f_3 = p^{(m,3)} b_3(t) \beta_{m,3} \frac{S_{m,3}^*}{S_{h,3}^*},$$

$$f_4 = p^{(h,1)} a_1 \beta_{h,1}, \quad f_5 = p^{(h,2)} a_2 \beta_{h,2}, \quad f_6 = p^{(h,3)} a_3 \beta_{h,3},$$

$$v_1 = d_{11} + \sum_{j=2}^{3} c_{j1}^I, \quad v_2 = d_{12} + \sum_{j=1, j\neq 2}^{3} c_{j2}^I, \quad v_3 = d_{13} + \sum_{j=1}^{2} c_{j3}^I, \quad v_4 = d_{21} + \sum_{j=2}^{3} c_{j1}^U,$$

$$v_5 = d_{22} + \sum_{j=1, j\neq 2}^{3} c_{j2}^U, \quad \text{and} \quad v_6 = d_{23} + \sum_{j=1}^{2} c_{j3}^U.$$

Then,

$$S_{h,1}^* = \frac{\alpha_{h,1}(\mu_{h,2} M_3 + c_{32}^S(\mu_{h,3} + c_{13}^S) + c_{12}^S M_3) + \alpha_{h,2}(c_{13}^S c_{32}^S + c_{12}^S M_3) + \alpha_{h,3}(c_{12}^S c_{23}^S + c_{13}^S M_2)}{\mu_{h,1}(M_3(\mu_{h,2} + c_{12}^S) + c_{13}^S c_{32}^S) + \mu_{h,3}(c_{32}^S M_1 + c_{31}^S(\mu_{h,2} + c_{12}^S)) + \mu_{h,2}(c_{21}^S M_3 + c_{23}^S c_{31}^S)},$$

$$S_{h,2}^* = \frac{\alpha_{h,1}(c_{23}^S c_{32}^S + c_{21}^S M_3) + \alpha_{h,2}(\mu_{h,1} M_3 + c_{31}^S(\mu_{h,3} + c_{23}^S) + c_{21}^S M_3) + \alpha_{h,3}(c_{21}^S c_{13}^S + c_{23}^S M_1)}{\mu_{h,1}(M_3(\mu_{h,2} + c_{12}^S) + c_{13}^S c_{32}^S) + \mu_{h,3}(c_{32}^S M_1 + c_{31}^S(\mu_{h,2} + c_{12}^S)) + \mu_{h,2}(c_{21}^S M_3 + c_{23}^S c_{31}^S)},$$

and

$$S^*_{h,3} = \frac{\alpha_{h,1}(c^S_{32}c^S_{21} + c^S_{31}M_2) + \alpha_{h,2}(c^S_{31}c^S_{12} + c^S_{32}M_1) + \alpha_{h,3}(\mu_{h,1}M_2 + c^S_{21}(\mu_{h,2} + c^S_{32}) + c^S_{31}M_2)}{\mu_{h,1}(M_3(\mu_{h,2} + c^S_{12}) + c^S_{13}c^S_{32}) + \mu_{h,3}(c^S_{32}M_1 + c^S_{31}(\mu_{h,2} + c^S_{12})) + \mu_{h,2}(c^S_{21}M_3 + c^S_{23}c^S_{31})},$$

with $M_1 = \mu_{h,1} + c^S_{21} + c^S_{31}, \quad M_2 = \mu_{h,2} + c^S_{12} + c^S_{32}, \quad M_3 = \mu_{h,3} + c^S_{13} + c^S_{23}$, as the components of the solution of the algebraic equation $M_h S^*_h = \alpha_h$.

The disease-free periodic solution is given by

$$E^+_0(t) = (S^*_{h,1}, S^*_{h,2}, S^*_{h,3}, 0, 0, 0, 0, 0, 0, 0, 0, 0, 0, S^*_{m,1}(t), S^*_{m,2}(t), S^*_{m,3}(t), 0, 0, 0).$$

An explicit solution for R_0 is difficult using the linear operator method (since finding the spectral radius of the monodromy matrix $\Phi_{F-V}(t)$, $\rho(\Phi_{F-V}(\omega))$ and solving the spectral radius for a λ_0 such that $\rho(\Phi_{F-V}(\omega)) = 1$ is challenging).

Instead, we will draw some conclusions by considering the situation when there is no human movement between the zones, that is, the migration rates matrices $C^\Pi = [c^\Pi_{i,j}] = 0$, $\Pi = S, I, U, T$ and $i, j = 1, 2, 3$, are all equal to zero. Then, the reproduction ratio R_0 for the model (8) is given by

$$R_0 = \max\{R_{0i}\}, \quad C^\Pi = 0, \tag{38}$$

where

$$R_{0i} = \sqrt{\frac{a_i[b_i]p^{(h,i)}p^{(m,i)}\beta_{h,i}\beta_{m,i}(d_{2i} - \pi_i\eta_{h,i})K_i[r_{m,i}]}{(d_{1i}d_{2i} - \eta_{h,i}\xi_{h,i})[\alpha_{m,i}][\mu_{m,i}]S^*_{h,i}}}, \tag{39}$$

is the local reproduction ratio for zone i, and

$$[\alpha_{m,i}] := \frac{1}{12}\int_1^{12} \alpha_{m,i}(t)dt, \quad [\mu_{m,i}] := \frac{1}{12}\int_1^{12} \mu_{m,i}(t)dt, \quad [b_i] := \frac{1}{12}\int_1^{12} b_i(t)dt$$

are the long-term average values of the continuous periodic functions $\alpha_{m,i}(t)$, $\mu_{m,i}(t)$ and $b_i(t)$, $i = 1, 2, 3$, respectively.

From Eq. (38), we note that $R_0 > 1$ does not mean that the disease becomes prevalent in all the zones. Since the zones are isolated, the behaviour in each zone is determined by the value of the respective local reproduction number R_{0i}. Indeed, when $\min R_{0i} > 1$, the disease-free periodic solution is unstable, and the disease may invade the populations. Also, when $R_0 < 1$, then all zones have a locally asymptotically stable disease-free periodic solution [37]. In addition, if there is human movement, the reproduction ratio R_0 depends on the travel rate of the infected humans and satisfies the following inequality [74]

$$\min\{R_{0i}\} \le R_0 \le \max\{R_{0i}\}, \quad 1 \le i \le n, \quad C^\Pi \neq 0. \tag{40}$$

5.3. Numerical simulation

The long-term behaviour of solutions of the system (8) are shown in Figures 7-11. The numerical values of the parameters are given in Table 2. Next, we numerically explore

the impact of human travel, and, in particular, of counterfeit antimalarial drug users, on disease transmission. We restrict our analysis to two main scenarios and discuss our results. The scenarios are:
(a) no travelling between zones
(b)four sub-cases of human travelling between the three zones: (i) all individuals travel irrespective of their epidemiological status, (ii) only susceptible humans, counterfeit and the effective antimalarial drug users travel, (iii) only susceptible and effective antimalarial drug users travel, (iv) only susceptible humans travel
while the per capita rate of infectious humans becoming counterfeit drug users η_h and the recrudescence rate ξ_h are varied(between 1, $\frac{30}{14}$ and $\frac{30}{7}$). The parameter η_h given by 1, $\frac{30}{14}$ and $\frac{30}{7}$ means it takes a month, two weeks and a week respectively, to transit from infectious human to counterfeit drug user. Also, the parameter ξ_h given by 1, $\frac{30}{14}$ and $\frac{30}{7}$ means it takes a month, two weeks and a week respectively, to transit from counterfeit drug user to infectious human due to recrudescence.

We illustrate the first scenario in Figure 7. Here, the long-term behaviour of the infectious humans, counterfeit antimalarial drug users and the infectious mosquitoes in the three isolated ecological zones are shown with $c_{i,j}^{\Pi} = 0$, $\Pi = S, I, U, T$ and $i, j = 1, 2, 3$ and, η_h and ξ_h are varied. Figure 7 shows that the infection is persistent in zones 2 and 3 but dies out in the long term in zone 1, where the graphs show that the infected populations initially increased in all three zones. However, for zone 1, the populations begin to decrease with the periodic fluctuations to the low values, and for zones 2 and 3, the populations settle into periodic fluctuation in the long term (see Figures 7(a)-(i)). Interestingly, we observe that the number of infected populations can decrease in zone 3 when $\eta_h = 1$ and $\xi_h = \frac{30}{7}$ (see Figures 7(g)-(i)). Also, the population of users of counterfeit drugs in each zone is the highest when $\eta_h = \frac{30}{7}$ and $\xi_h = \frac{30}{14}$ and the lowest when $\eta_h = 1$ and $\xi_h = \frac{30}{7}$ (see Figure 7).

Next, we show the second scenario of travelling between the three zones. In Figure 8, we show the long-term behaviour of infectious humans, counterfeit antimalarial drug users and infectious mosquitoes for the case where all humans irrespective of their epidemiological status can travel between zones without restrictions, with the travel rates $c_{12}^{\Pi} = 0.3, c_{13}^{\Pi} = 0.2, c_{21}^{\Pi} = 0.5, c_{23}^{\Pi} = 0.5, c_{31}^{\Pi} = 0.3, c_{32}^{\Pi} = 0.9$, $\Pi = S, I, U, T$, and the other parameter values are as in Figure 8. Figure 8 shows that the infection is persistent in each zone, and one positive periodic solution exists. However, we observe that the number of infected humans and mosquitoes is high in zones 1, 2 and 3 compared to Figure 7. Here, the populations of infectious humans, users of counterfeit drugs and infectious mosquitoes in zone 1 initially increase, then begin to decrease and settle (see Figures 8(a)-(c)). For zones 2 and 3, these populations also increase until they settle into periodic fluctuations (Figures 8(d)-(i)). Here also, we observe that the population of users of counterfeit drugs in each zone is highest when $\eta_h = \frac{30}{7}$ and $\xi_h = \frac{30}{14}$ and lowest when $\eta_h = 1$ and $\xi_h = \frac{30}{7}$ (in Figure 8).

Figure 9 illustrates the case where no infectious human can travel. However, counterfeit antimalarial drug users may be able to move freely between zones because they do not have clinical symptoms. We use the travel rates $c_{12}^{\Pi} = 0.3, c_{13}^{\Pi} = 0.2, c_{21}^{\Pi} = 0.5, c_{23}^{\Pi} = 0.5, c_{31}^{\Pi} = 0.3, c_{32}^{\Pi} = 0.9$, $\Pi = S, U, T$, travel matrices $C^I = 0$ and the parameter values as in Figure 7. Here, we observe that the graphs in Figure 9 are similar to the graphs in Figure 8, except that prevalence decreases in zones 1 and 3 but increases in zone 2 compared to the results in Figure 8.

In Figure 10, we illustrate the case when no infected human (i.e., infectious and counterfeit drug users) travels, using the travel rates $c_{12}^{\Pi} = 0.3, c_{13}^{\Pi} = 0.2, c_{21}^{\Pi} = 0.5, c_{23}^{\Pi} =$

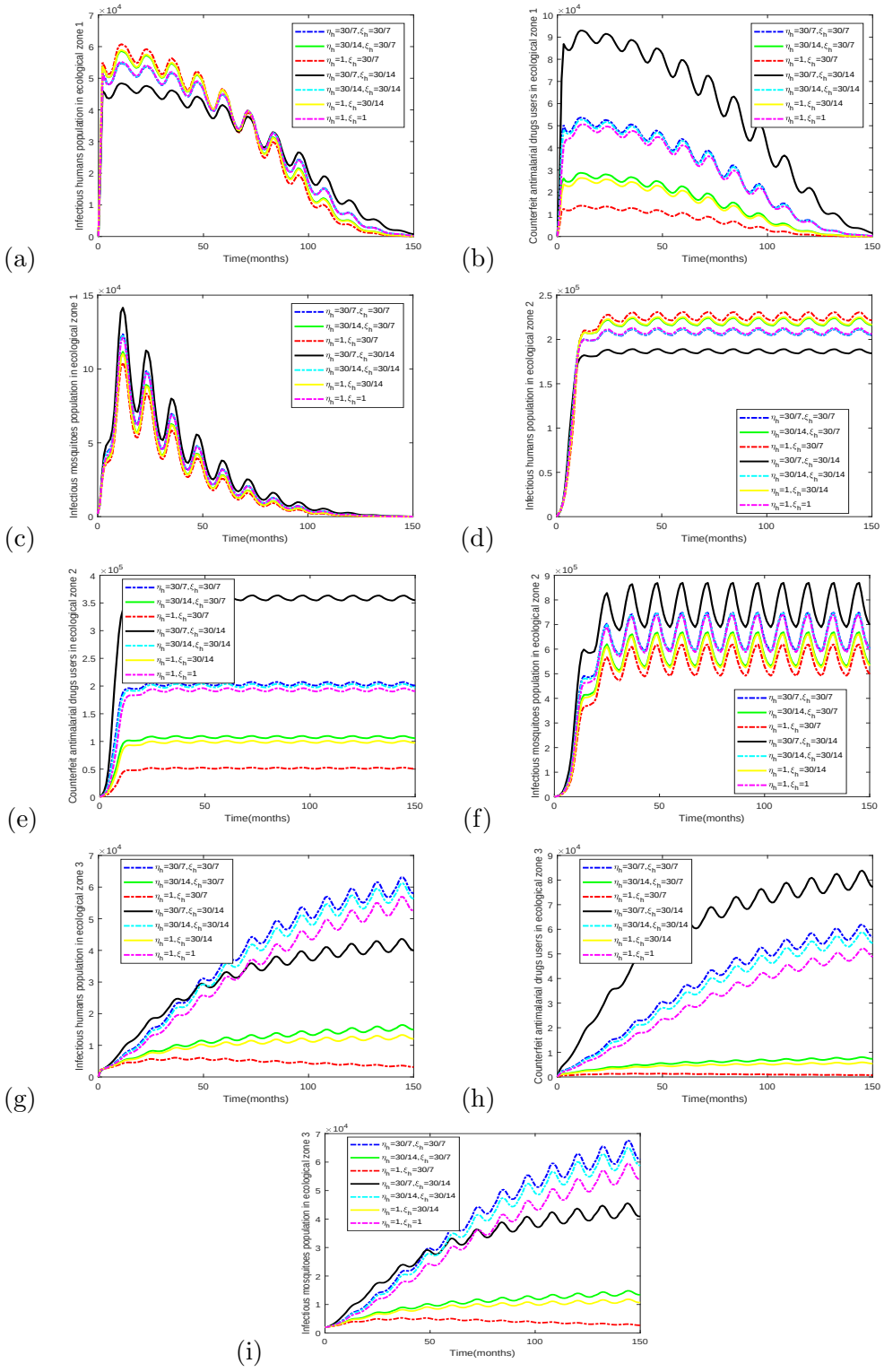

Figure 7. Simulation of the infectious humans, users of counterfeit drugs and infectious mosquitoes populations of the climate-based metapopulation malaria model (8) for the three ecological zones. Here, the zones are isolated such that no humans travel between the zones (i.e. $C^{\Pi} = 0$) and use initial conditions: $S_{h1} = 370000, I_{h1} = 100, U_{h1} = 100, T_{h1} = 100, S_{h2} = 1500000, I_{h2} = 100, U_{h2} = 100, T_{h2} = 100, S_{h3} = 2100000, I_{h3} = 100, U_{h3} = 100, T_{h3} = 100, S_{m1} = 1000000, I_{m1} = 2000, S_{m2} = 10000000, I_{m2} = 1000, S_{m3} = 6000000, I_{m3} = 2000$.

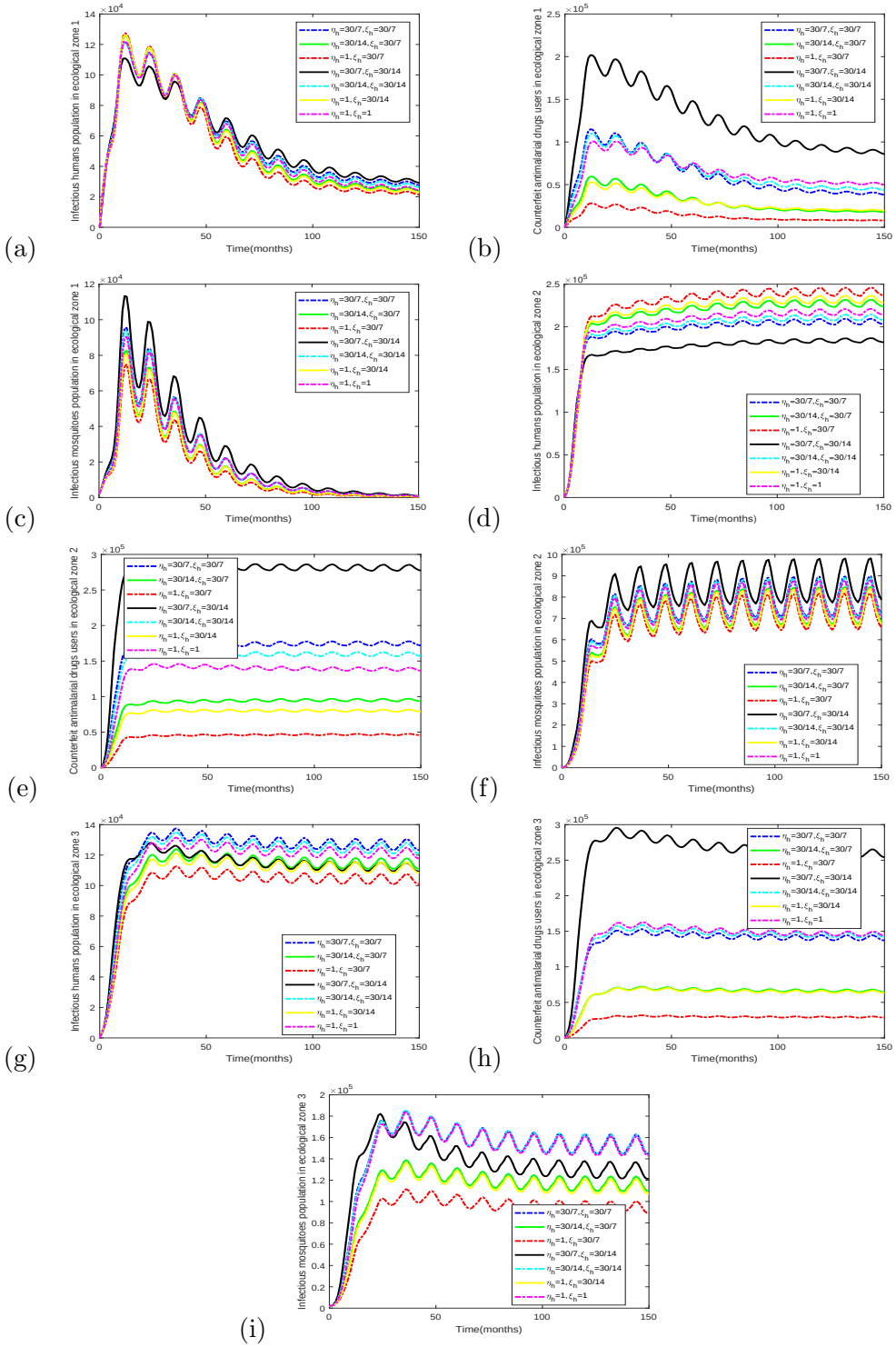

Figure 8. Simulation of the infectious humans, users of counterfeit drugs and infectious mosquito populations of the system (8) for the three ecological zones. Here, all humans move across the three zones. The travel rates are $c_{12}^{\Pi} = 0.3, c_{13}^{\Pi} = 0.2, c_{21}^{\Pi} = 0.5, c_{23}^{\Pi} = 0.5, c_{31}^{\Pi} = 0.3, c_{32}^{\Pi} = 0.9$, $\Pi = S, I, U, T$ and initial conditions: $S_{h1} = 370000, I_{h1} = 100, U_{h1} = 100, T_{h1} = 100, S_{h2} = 1500000, I_{h2} = 100, U_{h2} = 100, T_{h2} = 100, S_{h3} = 2100000, I_{h3} = 100, U_{h3} = 100, T_{h3} = 100, S_{m1} = 1000000, I_{m1} = 1000, S_{m2} = 10000000, I_{m2} = 1000, S_{m3} = 6000000, I_{m3} = 1000$. The parameters used are given in Table 2.

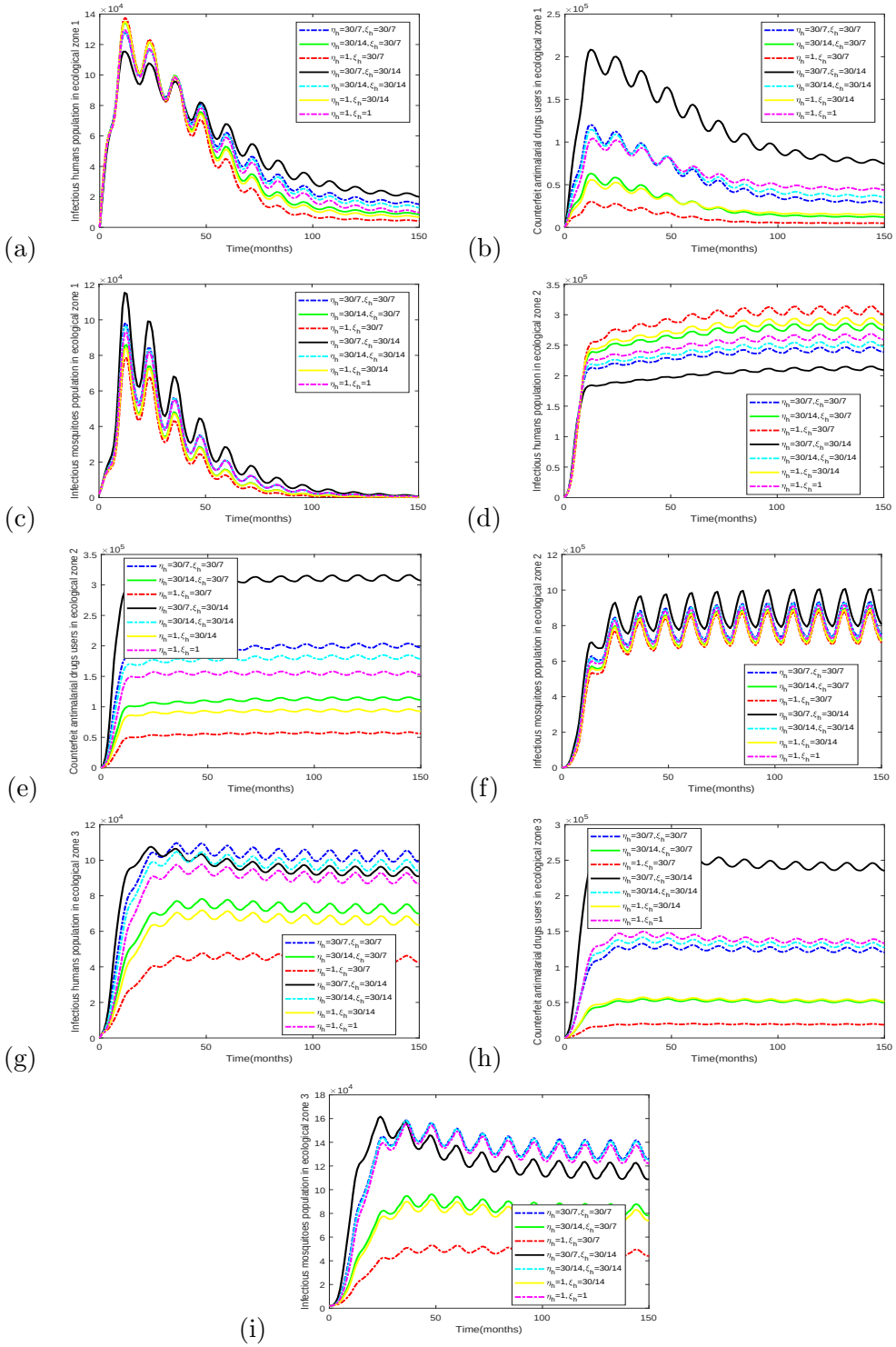

Figure 9. Graph of the system (8) with no movement of the infectious humans between the three zones. The travel rates and matrix are $c_{12}^{\Pi} = 0.3, c_{13}^{\Pi} = 0.2, c_{21}^{\Pi} = 0.5, c_{23}^{\Pi} = 0.5, c_{31}^{\Pi} = 0.3, c_{32}^{\Pi} = 0.9$, $\Pi = S, U, T$ and $C^I = 0$ respectively. Initial conditions: $S_{h1} = 370000, I_{h1} = 100, U_{h1} = 100, T_{h1} = 100, S_{h2} = 1500000, I_{h2} = 100, U_{h2} = 100, T_{h2} = 100, S_{h3} = 2100000, I_{h3} = 100, U_{h3} = 100, T_{h3} = 100, S_{m1} = 1000000, I_{m1} = 1000, S_{m2} = 10000000, I_{m2} = 1000, S_{m3} = 6000000, I_{m3} = 1000$. The parameters used are given in Table 2.

$0.5, c_{31}^{\Pi} = 0.3, c_{32}^{\Pi} = 0.9$, $\Pi = S, T$, and travel matrices $C^I = C^U = 0$. Here, the disease persists in zones 2 and 3 (see Figures 10(d)-(i)), but dies out in zone 1 in the long term (Figures 10(a)-(c)). For zone 1, the infectious humans, users of counterfeit drugs, and infectious mosquito populations initially increase but then converge to 0, undergoing periodic fluctuations (i.e., the disease-free periodic solution). For zone 2, the populations increase and settle into periodic fluctuations and for zone 3, the populations in the long term increase with periodic fluctuations when $\eta_h = \xi_h$, but begin to decrease when $\eta_h \neq \xi_h$. Comparing the results in Figure 10 with Figures 7 and 8, we note that the disease prevalence decreases in zones 1 and 3 and increases in zone 2. We also note that the population of users of counterfeit drugs in each zone is the lowest when $\eta_h = 1$ and $\xi_h = \frac{30}{7}$.

Finally, we consider the case when only susceptible individuals move between the zones. Here, Figure 11 shows that the infection persists in zones 2 and 3 but dies out in zone 1. However, we observe that the numbers of infected humans and mosquitoes are high in zones 2 and 3 as compared to Figure 7. The populations of infectious humans, users of counterfeit drugs and infectious mosquitoes in zone 1 initially increase, then begin to decrease until all converge to zero (Figures 11(a)-(c)). For zones 2 and 3, the populations also increase until they settle into periodic fluctuations (Figures 11(d)-(i)). Figure 11 indicates that the disease prevalence decreases in zones 1 and 3, and increases in zone 2 when compared with the results in Figure 8; also, the population of users of counterfeit drugs in each zone is the highest when $\eta_h = \frac{30}{7}$ and $\xi_h = \frac{30}{14}$ and lowest when $\eta_h = 1$ and $\xi_h = \frac{30}{7}$ (see Figures 11(a)-(i)). Considering the first and second scenarios of travelling in all three zones (see Figure 7 and Figures 8-11), we find that while introduction of movement of non-infected humans with infectious humans and/or counterfeit drug users enhances the survival of the disease by changing a disease-free zone into an endemic zone (Figures 8 and 9(a)-(c)), the movement of only non-infected humans can possibly make an endemic zone either disease free (Figures 10(g)-(i)) depending on the values of η_h and ξ_h, or endemic (Figures 11(g)-(i)). We notice that the long-term behaviour of the populations when users of counterfeit drugs travel across zones (in Figure 9) is similar to when both infectious humans and users of counterfeit drugs travel across zones (in Figure 8).

6. Discussion and Conclusion

Mathematical models that are based on key features relevant to infectious disease transmission can provide an important tool to understand the dynamics of transmission and the spread of the disease and, thus, provide suggestions and policies for disease control [71]. We formulated and analyzed a climate-based metapopulation malaria model which takes into account that (i) the mosquito life cycle, the local mosquito population and some entomological parameters relevant to malaria transmission are greatly influenced by climatic factors such as the rainfalls and temperatures [9, 14, 70]; (ii) human travel between spatially heterogenous environments also induce the translocation of parasites into other regions [37]; (iii) significant use of the ineffective drugs in some endemic malaria areas [7]. Our model was motivated by that considered in [34, 37, 51, 72, 73] but we extended it to address the time-periodic rates of birth, death and biting for the mosquito population in n ecological zones, the counterfeit and effective antimalarial drug users in the human population and human movement between the n ecological zones. We also allowed for human travel from one ecological zone to another. Such a model provides a better understanding of

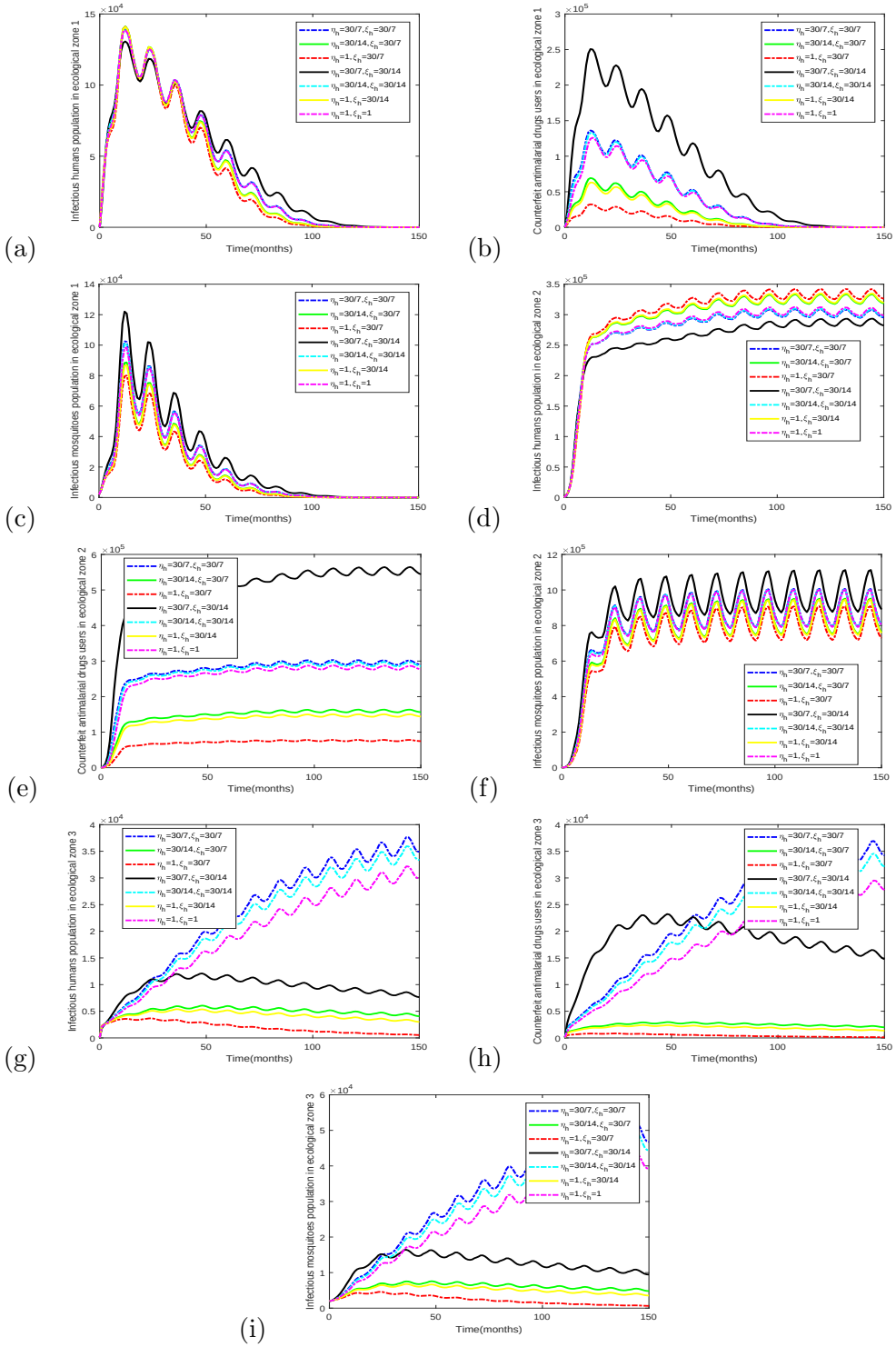

Figure 10. Simulation of the model (8) with the movement of only susceptible humans and effective antimalarial drug users between the three zones. The travel rates and matrices are $c_{12}^{\Pi} = 0.3, c_{13}^{\Pi} = 0.2, c_{21}^{\Pi} = 0.5, c_{23}^{\Pi} = 0.5, c_{31}^{\Pi} = 0.3, c_{32}^{\Pi} = 0.9$, $\Pi = S, T$ and $C^I = C^U = 0$, respectively. Initial conditions: $S_{h1} = 370000, I_{h1} = 100, U_{h1} = 100, T_{h1} = 100, S_{h2} = 1500000, I_{h2} = 100, U_{h2} = 100, T_{h2} = 100, S_{h3} = 2100000, I_{h3} = 100, U_{h3} = 100, T_{h3} = 100, S_{m1} = 1000000, I_{m1} = 1000, S_{m2} = 10000000, I_{m2} = 1000, S_{m3} = 6000000, I_{m3} = 1000$. The parameters used are given in Table 2.

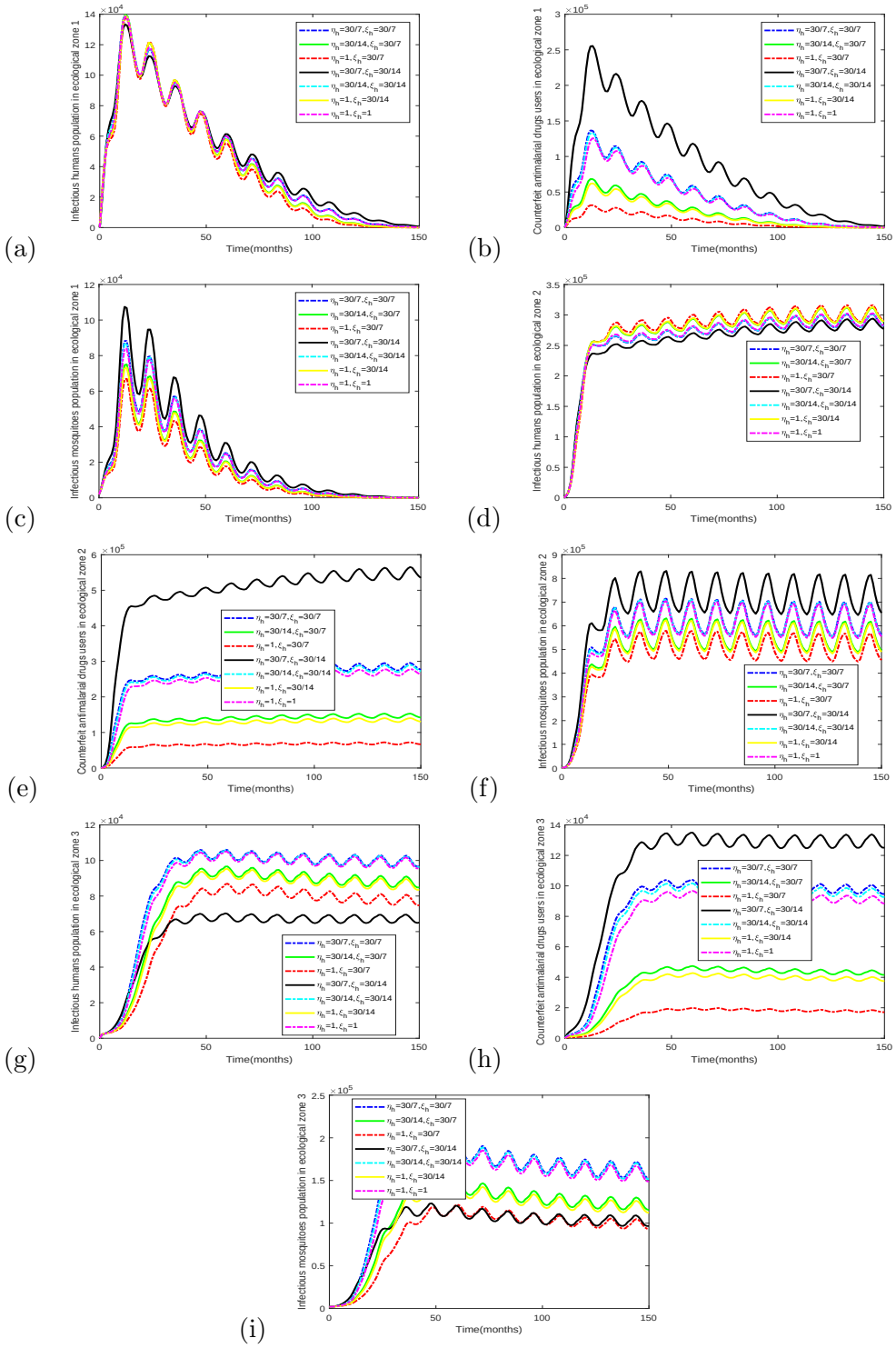

Figure 11. Simulation of system (8) for the three zones with movement of only susceptible humans. The travel rates and matrices are $c_{12}^S = 0.3, c_{13}^S = 0.2, c_{21}^S = 0.5, c_{23}^S = 0.5, c_{31}^S = 0.3, c_{32}^S = 0.9$ and $C^I = C^U = C^T = 0$ respectively. Initial conditions: $S_{h1} = 370000, I_{h1} = 100, U_{h1} = 100, T_{h1} = 100, S_{h2} = 1500000, I_{h2} = 100, U_{h2} = 100, T_{h2} = 100, S_{h3} = 2100000, I_{h3} = 100, U_{h3} = 100, T_{h3} = 100, S_{m1} = 1000000, I_{m1} = 1000, S_{m2} = 10000000, I_{m2} = 1000, S_{m3} = 6000000, I_{m3} = 1000$. The parameters used are given in Table 2.

the dynamics of malaria transmission and insights into designing control measures for antimalarial drugs, policies on migration, and the evaluation of the long-term effects of climate change on malaria.

By applying the theorem of the next generation operator, we showed the existence of the reproduction ratio R_0. We showed that the non-trivial disease-free equilibrium is locally asymptotically stable if $R_0 < 1$. Thus, if $R_0 < 1$, then malaria will be eliminated, and a small disease invasion will be cleared from the population. We illustrated the theory by considering a special case of malaria in three cities (i.e., Tamale, Kumasi and Accra) within three ecological zones of Ghana. By using published data about these cities and the formula related to the mosquito life cycle and the biting rate, estimates of all the constants and the periodic parameters were found. An explicit formula for the global R_0 for the three cities could not be obtained in the closed form, however, the local reproduction ratios for the individual cities (where there is no movement) were computed using the time-averaged parameters. The reproduction ratios for Tamale, Kumasi and Accra were calculated as 13, 1.8 and 0.7 respectively (when $\eta_h = 1$ and $\xi_h = 30/7$) and 2.707, 0.368 and 0.156 (when $\eta_h = 30/7$ and $\xi_h = 30/14$). For Accra, since $R_{0i} < 1$, the disease may be controlled if the migration is not allowed in the city, while for Tamale, the disease will persist since $R_{0i} > 1$. However, the disease may persist or go extinct in Kumasi depending on the value of η_h and ξ_h.

We numerically simulated the model to explore the impact of different movement situations on the long-term behaviour of the model when the per capita rate of infectious humans becoming counterfeit drug users η_h and the recrudescence rate ξ_h are varied. We observed that the climatic effect on the mosquitoes' birth, death and biting rates introduces fluctuations in the simulations. Our results showed that the movement between zones affects the disease prevalence in each zone, the local transmission dynamics of malaria, and possibly the global dynamics of the system. Our findings indicate that the impact of movement on disease transmission varies depending on whether the movement is by both the infected and non-infected humans or just non-infected humans. The former scenario always leads to an increase in the disease prevalence in the zones, while the latter can increase or decrease disease prevalence depending on the rate at which the infectious humans use counterfeit drugs and on the recrudescence rate. For example, the movement of only non-infected humans results in an endemic zone staying endemic (with decreased or increased prevalence) or becoming disease-free in the long run. On the other hand, the movement of non-infected humans with infected humans changed the disease-free status of a zone to a disease-persistent status. This implies that malaria may become endemic, even when the infectious humans are not travelling. In the case of non-infected humans travelling, the per capita rate at which the infectious humans become counterfeit drug users, and the recrudescence rate need to be considered.

We also observed that the population of counterfeit drug users in each zone is the highest when $\eta_h = \frac{30}{7}$ and $\xi_h = \frac{30}{14}$ and the lowest when $\eta_h = 1$ and $\xi_h = \frac{30}{7}$. Ghana has a significant proportion of malaria-infected humans that use counterfeit drugs [5, 6], and our numerical results suggest that the reason for the endemicity of malaria in all regions and zones of Ghana could be due to the unregulated movement of both infected and non-infected humans.

Our model has helped to expose qualitatively the overall effect of human movement on malaria transmission in a periodic environment. The information obtained on the impact of human travel between zones on disease epidemics and antimalarial drugs can be used to guide policies on travel. Also, the results strongly support the thesis

that the sale, importation, trade or manufacture of counterfeit drugs should be banned and offenders punished. This will ensure only high-quality drugs are used.

Calculating the reproduction ratio for some vector-host periodic models can be challenging, and hence, the impact of mosquito mobility across zones on malaria transmission is often neglected. To alleviate this difficulty, we used the time-average estimates for the reproduction ratio in this paper. This, however, has been found sometimes to underestimate the reproduction number and the risk of the infection [44, 59], and our results should be viewed with this understanding. We also note that if the connected cities are near each other, then the influence of the mosquitoes can also move across the boundaries, and the impact of these migrations on malaria transmission cannot be ignored. Hence, incorporating mosquito migration into the model would be biologically more reasonable. In future work, we plan to modify the model to incorporate mosquito mobility, unequal travel matrices, and other realistic forms of movement and use other methods to calculate the reproduction ratio for periodic coefficients.

Acknowledgments

All sources of funding of the study must be disclosed

Disclosure statement

The authors declare there is no conflict of interest.

Funding

The authors declare there was no funding for this study.

References

[1] World Health Organization, World Malaria Report 2021. *World Health Organization*,Geneva, Switzerland, 2021. Licence: CC BY-NC-SA 3.0 IGO.

[2] World Health Organization, World Malaria Report 2020. *World Health Organization*,Geneva, Switzerland, 2020. Licence: CC BY-NC-SA 3.0 IGO.

[3] World Health Organization, World Malaria Report 2018. *World Health Organization*,Geneva, Switzerland, 2018. Licence: CC BY-NC-SA 3.0 IGO.

[4] World Health Organization, World Malaria Report 2017. *World Health Organization*,Geneva, Switzerland, 2017. Licence: CC BY-NC-SA 3.0 IGO.

[5] R. B. Awuah, P. Y. Asante, L. Sakyi, A. A. E. Biney, M. K. Kushitor, F. Agyei, A. D-G. Aikins, Factors associated with treatment-seeking for malaria in urban poor communities in Accra, Ghana, *Malaria Journal*,**17**(2018). https://doi.org/10.1186/s12936-018-2311-8.

[6] R. C. Brenyah, D. N. M. Osakunor, R. K. D. Ephraim, Factors influencing urban malaria: a comparative study of two communities in the Accra Metropolis, *African Health Sciences*,**13**(2013),992–998.

[7] J. P. Renschler, K. M. Walters, P. N. Newton, R. Laxminarayan, Estimated under-five deaths associated with poor-quality antimalarials in Sub-Saharan Africa, *The American Journal of Tropical Medicine and Hygiene* **92**(2015),119–126.

[8] P. N. Newton, M. D. Green, D. C. Mildenhall, A. Plancon, H. Nettey, L. Nyadong, et al., Poor quality vital antimalarials in Africa–an urgent neglected public health priority, *Malaria Journal* **10**(2011). https://doi.org/10.1186/1475-2875-10-352.

[9] A. Githeko, J. Ayisi, P. Odada, F. Atieli, B. Ndenga, J. Githure, G. Yan, Topography and malaria transmission heterogeneity in western Kenya high-lands: prospects for focal vector control, *Malaria Journal* **5**(2006).

[10] P. W. Gething, A. P. Patil, D. L. Smith, A. Carlos, C. A. Guerra, I. R. F. Elyazar, et al., A new world malaria map. Plasmodium falciparum endemicity in 2010, *Malaria Journal* **10**(2011).

[11] V. Robert, K. Macintyre, J. Keating, J. F. Trape, J. B. Duchemin, M. Warren, J. C. Beier, Malaria transmission in urban Sub-Saharan Africa, *The American Journal of Tropical Medicine and Hygiene* **68**(2003),169–176.

[12] P. E. Parham, E. Michael, Modeling the effects of weather and climate change on malaria transmission, *Environ. Health Perspect.* **118**(2010),620-626.

[13] P. E. Parham, E. Michael, Modeling climate change and malaria transmission, *Advances in Experimental Medicine and Biology* **673**(2010),184–199.

[14] S. F. Rumisha, T. Smith, S. Abdulla, H. Masanja, P. Vounatsou, Modelling heterogeneity in malaria transmission using large sparse spatio-temporal entomological data, *Global Health Action* **7**(2014). http://dx.doi.org/10.3402/gha.v7.22682.

[15] K. Badu, C. Brenya, C. Timmann, R. Garms, T. F. Kruppa, Malaria transmission intensity and dynamics of clinical malaria incidence in a mountainous forest region of Ghana, *Malaria World Journal* **4**(2013).

[16] S. C. K. Tay, S. K. Danuor, D. C. Mensah, G. Acheampong, H. H. Abuquah, A. Morse, et al., Climate variability and malaria incidence in peri-urban, urban and rural communities around Kumasi, Ghana: a case study at three health facilities; Emena, Atonsu and Akropong, *International Journal of Parasitology Research* **4**(2012),83–89.

[17] L. E. G. Mboera, K. P. Senkoro, B. K. Mayala, S. F. Rumisha, R. T. Rwegoshora, M. R.S. Mlozi, et al., Spatio-temporal variation in malaria transmission intensity in five agro-ecosystems in Mvomero district, Tanzania, *Geospat Health* **4**(2010).

[18] *USAID/FRHP/PMI/NMCP/JSI Research and Training Inc.*, Report of the Ghana Urban Malaria Study, 2013.

[19] P. M. De Silva, J. M. Marshall, Factors Contributing to Urban Malaria Transmission in Sub-Saharan Africa: A Systematic Review, *Journal of Tropical Medicine* **2012**(2012). https://doi:10.1155/2012/819563.

[20] *Ghana Statistical Service, Accra*, Ghana Multiple Indicator Cluster Survey with an Enhanced Malaria Module and Biomarker 2011 Final Report, 2011.

[21] T. Awine, K. Malm, N. Y. Peprah, S. P. Silal, Spatio-temporal heterogeneity of malaria morbidity in Ghana: analysis of routine health facility data, *PLOS ONE* **13**(2018). https://doi.org/10.1371/journal.pone.0191707.

[22] P. B. Bloland, Drug resistance in malaria, *World Health Organization*, Geneva, Switzerland, 2001. http://www.who.int/csr/resources/publications/drugresist/malaria.pdf.

[23] M. Baragatti, F. Fournet, M. C. Henry, S. Assi, H. Ouedraogo, C. Rogier, G. Salem, Social and environmental malaria risk factors in urban areas of Ouagadougou, Burkina Faso, *Malaria Journal* **8**(2009).

[24] S. I. Hay, C. A. Guerra, A. J. Tatem, P. M. Atkinson, R. W. Snow, Urbanization, malaria transmission and disease burden in Africa, *Nat Rev Microbiol.* **3**(2005)81–90.

[25] S. T. Stoddard, A. C. Morrison, G. M. Vazquez-Prokopec, V. P. Soldan, T. J. Kochel, U. Kitron, J. P. Elder, T. W. Scott, The role of human movement in the transmission of vector-borne pathogens, *PLoS Negl Trop Dis* **3**(2009)599–653. doi:10.1371/journal.pntd.0000481.

[26] S. Kasasa, V. Asoala, L. Gosoniu, F. Anto, M. Adjuik, C. Tindana, et al., Spatio-temporal malaria transmission patterns in Navrongo demographic surveillance site, Northern Ghana, *Malaria Journal* **12**(2013).

[27] D. Tchouassi, I. A. Quakyi, E. A. Addison, K. M. Bosompem, M. D. Wilson, M. A. Ap-

pawu, et al., Characterization of malaria transmission by vector populations for improved interventions during the dry season in the Kpone-on-Sea area of coastal Ghana, *Parasites & Vectors* **5**(2012).

[28] N. Ng'andu, T. E. Watts, J. R. Wray, C. Chela, B. Zulu, Some risk factors for transmission of malaria in a population where control measures were applied in Zambia, *East African Medical Journal* **66**(1989),728-737.

[29] A. Ejercito, C. M. Urbino, Flight range of gravid and newly emerged Anopheles, *Bulletin World Health Organization* **3**(1951),663–671. 1951.

[30] World Health Organization, Dengue control, *World Health Organization*, Geneva, Switzerland, 2018. http://www.who.int/denguecontrol/mosquito/en/.

[31] S. Ruan, J. Wu, Modeling the spatial spread of communicable diseases with animal hosts, in Cantrell RS, Cosner C, Ruan S (eds.), *Spatial Ecology*, Chapman Hall/CRC Press, Taylor and Francis Group, (2010),293–315.

[32] C. Cosner, J. C. Beier, R. S. Cantrell, D. Impoinvil, L. Kapitanski, M. D. Potts, A. Troyo, S. Ruan, The effects of human movement on the persistence of vector-borne diseases, *Journal of Theoretical Biology* **258**(2009),550–560. https://doi:10.1016/j.jtbi.2009.02.016.

[33] C. Cosner, Models for the effects of host movement in vector borne disease systems, *Mathematical Biosciences* **270**(2015),192–197. https://doi.org/10.1016/j.mbs.2015.06.015.

[34] Y. Xiao, X. Zou, Transmission dynamics for vector-borne diseases in a patchy environment, *Journal of Mathematical Biology* **69**(2014),113–146. https://doi:10.1007/s00285-013-0695-1.

[35] J. Arino, Diseases in metapopulations in *Modeling and dynamics of infectious diseases* **11**, World Scientific Publishing, Singapore,(2009), 65–123.

[36] L. Sattenspiel, The geographic spread of infectious diseases: models and applications (with contributions from Alun Lloyd) **5**, Princeton University Press, (2009). https://doi.org/10.1515/9781400831708.237.

[37] J. Arino, A. Ducrot, P. Zongo, A metapopulation model for malaria with transmission-blocking partial immunity in hosts, *Journal of Mathematical Biology* **64**(2012),423–448. https://doi:10.1007/s00285-011-0418-4.

[38] O. Prosper, N. Ruktanonchai, M. Martcheva, Assessing the role of spatial heterogeneity and human movement in malaria dynamics and control, *Journal of Theoretical Biology* **303**(2012),1–14. https://doi:10.1016/j.jtbi.2012.02.010.

[39] T. Bakary, S. Boureima, T. Sado, A mathematical model of malaria transmission in a periodic environment, *Journal of Biological Dynamics* **12**(2014),400–432.

[40] K. Okuneye, A. B. Gumel, Analysis of a temperature-and rainfall-dependent model for malaria transmission dynamics, *Mathematical Biosciences* **287**(2017),72-92. http://dx.doi.org/10.1016/j.mbs.2016.03.013.

[41] G. J. Abiodun, P. Witbooi, K. O. Okosun, Modelling the impact of climatic variables on malaria transmission, *Hacettepe Journal of Mathematics and Statistics* **47**(2018),219–235.

[42] F. B. Agusto, A. B. Gumel, P. E. Parham, Qualitative assessment of the role of temperature variations on malaria transmission dynamics, *Journal of Biological Systems* **23**(2015). https://doi.org/10.1142/S0218339015500308.

[43] E. T. Ngarakana-Gwasira, C. P. Bhunu, M. Masocha, E. Mashonjowa, Assessing the Role of Climate Change in Malaria Transmission in Africa, *Malaria Research and Treatment* **2016**(2016). http://dx.doi.org/10.1155/2016/7104291.

[44] X. Wang, X-Q. Zhao, A climate-based malaria model with the use of bed nets, *Journal of Mathematical Biology* **77**(2018),1–25. https://doi.org/10.1007/s00285-017-1183-9.

[45] D. Gao, Y. Lou, S. Ruan, A periodic Ross-MacDonald model in a patchy environment, *Discrete and Continous Dynamical Systems Series B* **19**(2014),3133–3145.

[46] B. A. Danquah, F. Chirove, J. Banasiak, Controlling malaria in a population accessing counterfeit antimalarial drugs. Mathematical Biosciences and Engineering, **20(7)**(2023), 11895–11938.

[47] P. Van den Driessche, J. Watmough, Reproduction numbers and sub-threshold endemic equilibria for compartmental models of disease transmission, *Mathematical Biosciences*

180(2002),29–48.
[48] W. Wang, X-Q. Zhao, Threshold dynamics for compartmental epidemic models in periodic environments, *Journal of Dynamics and Differential Equations* **20**(2008),699–717.
[49] World Health Organization, Guidelines for the treatment of malaria-3rd edition, *World Health Organization*, Geneva, Switzerland, 2015. http://www.who.int/malaria/publications/world-malaria-report-2015/report/en/.
[50] D. Moulay, M. A. A. Alaoui, H. Kwon, Optimal control of Chikunkunya disease: Larvae reduction, treatment and prevention, *Mathematical Biosciences and Engineering* **9**(2012),369–393. http://doi:10.3934/mbe.2012.9.369.
[51] F. Zhang, X-Q. Zhao, A periodic epidemic model in a patchy environment, *Journal of Mathematical Analysis and Application* **325**(2007),496–519.
[52] E. A. Mordecai, K. P. Paaijmans, L. R. Johnson, C. Balzer, T. Ben-Horin, E. Moor, et al., Optimal temperature for malaria transmission is dramatically lower than previously predicted, *Ecology letters* **16**(2013),22–30.
[53] H. L. Smith, Monotone Dynamical Systems: An Introduction to the Theory of Competitive and Cooperative Systems, *Mathematical Surveys and Monographs* **41**, A.M.S., Providence, RI, 1995.
[54] H. L. Smith, P. Waltman, The Theory of the Chemostat, *Cambridge University Press*, Cambridge, 1995.
[55] J. K. Hale, H. Koçak, Dynamics and bifurcations, *Texts in Applied Mathematics*, Springer-Verlag, New York, 1991.
[56] X-Q. Zhao, Dynamical Systems in Population Biology, *Springer-Verlag*, New York, 2003.
[57] A. Berman, R. J. Plemmons, Nonnegative matrices in the mathematical sciences, *SIAM* **9**, 1994.10.1137/1.9781611971262
[58] H. R. Thieme, Persistence under relaxed point-dissipativity with application to an endemic model, *SIAM Journal on Applied Mathematics* **24**(1993),407–435.
[59] C. D. Mitchell, Reproductive Numbers for Periodic Epidemic Systems. Ph.D. thesis, University of Texas at Arlington, USA.
[60] *World Population Review*, Population of cities in Ghana, 2018. http://worldpopulationreview.com/countries/ghana-population/cities/.
[61] *National Malaria Control Program, UHAS-Ghana, AngloGold AMCP-Ghana, WHO-Ghana, Wellcome Trust Programme-Kenya*, An epidemiological profile of malaria and its control in Ghana, 2013. https://www.linkmalaria.org/sites/www.linkmalaria.org/files/content/country/profiles/Ghana-epi-report2014.
[62] *Ghana Health Service*, Ghana Health Service Annual Report, 2016. https://www.ghanahealthservice.org/downloads/GHS_ANNUAL_REPORT_2016_n.pdf.
[63] J. B. Hall, M. D. Swaine, *Distribution and ecology of vascular plants in a tropical rain forest. forest vegetation in Ghana*, Springer, Netherlands, 1981. http://dx.doi.org/10.1007/978-94-009-8650-3.
[64] C. Csanyi, The ecosystems of Ghana, *Sciencing*, 2017. https://sciencing.com/ecosystems-ghana-13438.html.
[65] *Weather Atlas*, Monthly weather forecast and Climate Tamale, Ghana, 2002-2022, 2022. https://www.weather-atlas.com/en/ghana/tamale-climate.
[66] *Weather Atlas*, Monthly weather forecast and Climate Accra, Ghana, *Weather Atlas*, 2002-2022. https://www.weather-atlas.com/en/ghana/accra-climate.
[67] *Weather Atlas*, Monthly weather forecast and Climate Kumasi, Ghana, *Weather Atlas*, 2002-2022. https://www.weather-atlas.com/en/ghana/kumasi-climate.
[68] *Central Intelligence Agency (US)*, Africa-Ghana, 2018. https://www.cia.gov/library/publications/the-world-factbook/geos/print-gh.html.
[69] *USAID - President's Malaria Initiative*, Ghana Malaria Operational Plan FY 2018, USAID/NMCP, 2018. https://www.pmi.gov/docs/default-source/default-document-library/malaria-operational-plans/fy-2018/fy-2018-ghana-malaria-operational-plan.pdf?sfvrsn=5. Accessed: 17/12/2018.

[70] P. E. Parham, D. Pople, C. Christiansen-Jucht, S. Lindsay, W. Hinsley, E. Michael, Modeling the role of environmental variables on the population dynamics of the malaria vector anopheles gambiae sensu stricto, *Malaria Journal* **11**(2012).
[71] Y. Lou, X-Q. Zhao, A climate-based malaria transmission model with structured vector population, *SIAM Journal on Applied Mathematics* **70**(2010),2023–44.
[72] G. A. Ngwa, W. Shu, A mathematical model for endemic malaria with variable human and mosquito populations, *Mathematical and Computer Modelling* **32**(2000),747–63.
[73] H-F. Huo, G-M. Qiu, Stability of a mathematical model of malaria transmission with relapse, *Abstract and Applied Analysis* **2014**(2014).
[74] P. van den Driessche, Spatial structure: Patch models in *Mathematical Epidemiology. Lecture Notes in Mathematics, vol 1945*(eds. F. Brauer, P. van den Driessche P, J. Wu). Springer, Berlin, Heidelberg,(2008), 179–189.

7. Appendix

The equation (11) is a Bernoulli equation. Dividing (11) by $N_{m,i}^2$ gives

$$\frac{\dot{N}_{m,i}}{N_{m,i}^2} = r_{m,i}(t)\frac{1}{N_{m,i}} - \frac{\alpha_{m,i}(t)}{K_i}. \tag{41}$$

Let $v = N_{m,i}^{-1}$ and $\dot{v} = -\frac{\dot{N}_{m,i}}{N_{m,i}^2}$. Substituting v and $\dot{v}$ into (41) gives

$$\dot{v} + r_{m,i}(t)v = \frac{\alpha_{m,i}(t)}{K_i}. \tag{42}$$

Note that Eq. (42) is a first order linear differential equation. Multiplying (42) by the integrating factor $u(t) = e^{\int_0^t r_{m,i}(\tau)d\tau}$ gives

$$\begin{aligned}
\left(e^{\int_0^t r_{m,i}(\tau)d\tau}v\right)' &= \frac{\alpha_{m,i}(t)}{K_i}e^{\int_0^t r_{m,i}(\tau)d\tau}, \\
e^{\int_0^t r_{m,i}(\tau)d\tau}v &= \int_0^t \frac{\alpha_{m,i}(\tau)}{K_i}e^{\int_0^z r_{m,i}(\tau)d\tau}d\tau + C, \\
v &= \frac{e^{-\int_0^t r_{m,i}(\tau)d\tau}}{K_i}\left[\int_0^t \frac{\alpha_{m,i}(\tau)}{K_i}e^{\int_0^z r_{m,i}(\tau)d\tau}d\tau + C\right].
\end{aligned}$$

Since $v = N_{m,i}^{-1}$,

$$N_{m,i} = \frac{e^{\int_0^t r_{m,i}(\tau)d\tau}}{\int_0^t \frac{\alpha_{m,i}(\tau)}{K_i}e^{\int_0^z r_{m,i}(\tau)d\tau}d\tau + C}. \tag{43}$$

Applying the initial condition $N_{m,i}(0) = N_{m,i_0}$, we get

$$N_{m,i_0} = \frac{1}{C} \Rightarrow C = \frac{1}{N_{m,i_0}}.$$

Hence,

$$N_{m,i} = \frac{e^{\int_0^t r_{m,i}(\tau)d\tau}}{\int_0^t \frac{\alpha_{m,i}(\tau)}{K_i} e^{\int_0^z r_{m,i}(\tau)d\tau} d\tau + \frac{1}{N_{m,i_0}}}.$$

Further simplification gives the solution,

$$N_{m,i}(t) = \frac{K_i N_{m,i}(0) e^{\int_0^t r_{m,i}(\tau)d\tau}}{N_{m,i}(0) \int_0^t \alpha_{m,i}(\tau) e^{\int_0^z r_{m,i}(\tau)d\tau} d\tau + K_i}. \quad (44)$$